

JOET: Sustainable Vehicle-assisted Edge Computing for Internet of Vehicles

Wei Huang, Neal N. Xiong, *Senior Member, IEEE*, Shahid Mumtaz, *Senior Member, IEEE*

Abstract—Task offloading in Internet of Vehicles (IoV) involves numerous steps and optimization variables such as: where to offload tasks, how to allocate computation resources, how to adjust offloading ratio and transmit power for offloading, and such optimization variables and hybrid combination features are highly coupled with each other. Thus, this is a fully challenge issue to optimize these variables for task offloading to sustainably reduce energy consumption with load balancing while ensuring that a task is completed before its deadline. In this paper, we first provide a Mixed Integer Nonlinear Programming Problem (MINLP) formulation for such task offloading under energy and deadline constraints in IoV. Furthermore, in order to efficiently solve the formulated MINLP, we decompose it into two subproblems, and design a low-complexity Joint Optimization for Energy Consumption and Task Processing Delay (JOET) algorithm to optimize selection decisions, resource allocation, offloading ratio and transmit power adjustment. We carry out extensive simulation experiments to validate JOET. Simulation results demonstrate that JOET outperforms many representative existing approaches in quickly converge and effectively reduce energy consumption and delay. Specifically, average energy consumption and task processing delay have been reduced by 15.93% and 15.78%, respectively, and load balancing efficiency has increased by 10.20%.

Index Terms—Vehicular Edge Computing (VEC), Task offloading, Transmit power adjustment, Load balancing.

I. INTRODUCTION

THE Internet of Vehicles (IoV) has gained more attentions for researchers than ever before [1]–[3]. On the one hand, the number of vehicles has grown rapidly which can provide more service [4], [5]. On the other hand, more and more Internet of Things Devices (IoTDs) are deployed in demand to sense data [6], [7], communicate and perform tasks collaboratively, thus promoting the development of IoV based applications [6], [8]. According to the IoT Analytics, the number of IoTDs worldwide is expected to reach 22 billion by 2025 [8]. In order to make these massive, hardware-simple, and short communication range IoTDs can be cost-effective to connect to the Internet. Employing Mobile Vehicles (MVs) as the relay to connect IoTDs to the Internet is a low-cost and effective method in which when MVs enter communication range of IoTDs [9], IoTDs can upload their data or tasks to

the Internet via MVs [10], [11]. Especially in smart city, such way has a huge sustainability advantage because IoTDs can access the Internet conveniently and at low cost due to the large scale and wide distribution of vehicles [12].

Reviewing previous researches, task offloading in IoV mainly research offloading tasks of vehicles to Edge Servers (ESs). However, the widely deployed IoTDs in smart cities have a more urgent need for task offloading [13]–[15]. Relatively speaking, MVs have stronger computing power and communication capabilities, so they can upload their tasks to ESs at any time during the movement for offloading [9], [16]. Once deployed, IoTDs cannot be moved like MVs. Unless there are ESs available for offloading within communication range of IoTDs, tasks from IoTDs can only be offloaded through MVs as the relay node [9], [16]. These IoTDs can be deployed in areas that need to be monitored, such as Supervisory Control And Data Acquisition (SCADA) systems, so they have broad application prospects [17]. Therefore, offloading tasks from a huge number of IoTDs is more challenging and more valuable than the aforementioned task offloading of vehicles.

However, task offloading in such semi-connected networks which is studied in this paper is more challenging due to follow reasons.

(1) First, task offloading for IoTDs involves more steps and decisions, so the problem is more complicated. Tasks of IoTDs needs to be uploaded to MVs, and the decision that the MV needs to make after receiving the task is to complete the task by itself, or offload it to the ES. Not only that, in each step, we need to make a decision for the participants in task offloading. These decisions mainly include whether the task is to be offloaded? What is the ratio of offloaded the task? How much transmit power is applied? What are resources allocated to the task? Since each step affects the subsequent decisions, and each decision affects each other, the problem to be solved in this article is very complicated.

(2) Solving the optimization problem is quite challenging. The task offloading goals of IoTDs are as follow: (a) Time to complete the task is as small as possible; (b) Energy consumption of the network is as small as possible; (c) Network load balancing. Time to complete the task includes communication delay and computation delay. Then, resources allocated to the task are limited by the following factors. The first is resources of the task executor itself. If the task executor has more resources, the resources that can be allocated are more, and computation delay is smaller. Secondly, the network needs to balance the load of servers. Otherwise, it will lead to the limited resources that can be allocated to the task, which

This work was supported by the National Natural Science Foundation of China (62072475, 61772554) (*Corresponding author: Neal N. Xiong).

W. Huang is with School of Computer Science and Engineering, Central South University, ChangSha 410083 China. (e-mail: csu_hw@csu.edu.cn).

N. N. Xiong is with the Department of Mathematics and Computer Science, Northeastern State University, OK, 74464, USA. (e-mail: xiongnaihue@gmail.com).

S. Mumtaz is with the Instituto de Telecomunicações, Portugal, 1049-001 Aveiro, Portugal. (e-mail: smumtaz@av.it.pt).

increases the task processing delay [18].

It can be concluded that the goals of IoTDS task offloading in this article are to reduce task processing delay and total energy consumption with load balancing while ensuring task completion. Limitations are as follows: First, it is used to ensure that tasks can only be offloaded to one place; and the allocated resources need to meet the minimum task processing delay; and the sum of the total resources allocated to multiple tasks by an edge server cannot exceed the total amount of resources of the server; Finally, ratio of the offloaded computation bits does not exceed 1. Thus, offloading a task requires optimizing selection decisions, resource allocation, offloading ratio and transmit power adjustment. There is a highly complex coupling between optimization variables and hybrid combination features, so it is extremely challenging to solve such the task offloading problem. This paper formulates the above task offloading problem as a Mixed Integer Non-Linear Programming (MINLP) problem to better solve this problem. In summary, the main contributions of this paper are summarized as follows:

- We first propose the task offloading issue for IoTDS through MVs in IoV. Unlike previous studies that only studied task offloading on MVs, we have raised the issue of how to sustainably offload tasks from IoTDS through MVs. We further formulate the problem of minimizing energy consumption and task processing delay as a system utility maximization problem, and then transform the problem into a MINLP with consideration of load balancing.
- We propose a Joint Optimization for Energy consumption and Task processing delay (JOET) algorithm to effectively solve the proposed MINLP to minimize energy consumption and task processing delay. Our proposed JOET first determines selection decisions under given resource allocation, offloading ratio and transmit power, and then optimizes the three variables under obtained selection decisions. The optimization solution with less overhead can be found by repeating the above optimization steps until convergence.
- We carry out extensive simulation experiments to validate our proposed JOET. Simulation results demonstrate that JOET outperforms many representative existing algorithms in quickly converge and effectively reduce energy consumption and delay. Specifically, the average energy consumption and task processing delay have been reduced by 15.93% and 15.78%, respectively, and the load balancing efficiency has increased by 10.20%.

The rest of the paper is organized as follows. In Section II, we review related works. Section III introduces the system model and problem description, while Section IV presents the problem decoupling and the solution. We present the performance analysis in Section V. Finally, Section VI concludes this paper and introduce future work.

II. RELATED WORKS

Task offloading is to solve the lack of computing power of some devices in the current network, and computation

resources of other devices are sufficient and available to complement each other, so as to make full use of network resources [9], [19]. On the one hand, for IoTDS with insufficient computing power such as sensor nodes and phones, MVs cannot meet the needs of latency-intensive tasks [20], [21]. On the other hand, a large number of Edge Servers (ESs) with powerful computing capabilities are deployed at the edge of the network, which can process tasks from the edge network nearby. There are a lot of studies focused on task offloading [9], [16], [18], [22]. The task offloading mainly involves the following aspects: (1) where to offload [9]; (2) Resource allocation [18], [22]; (3) Transmission rate adjustment [16].

The issue for where to offload refers to where tasks is generated, and where they are offloaded for computing. There are many devices that generate tasks, and offload strategies of tasks generated by different devices are different. The most studied among them is that IoTDS in the network edge can directly communicate with the Internet for task offloading. In such the task offloading, the network is divided into 3 layers [23]: (a) Things Layer, (b) Fog Layer, (c) Cloud. The task is generated by IoTDS in the things layer. Due to the relatively weak computing power of IoTDS, they cannot meet the task requirements, and the task needs to be offload to Fog layer or cloud with more computation resources [23]. In such three-layer task offloading, some researchers have proposed game-based task offloading strategies, whose goal is to make these three layers maintain a more balanced load through game to maximize the utilization of network resources [19], [23]. Further, Yu *et al.* [23] think that different tasks have different computation requirements. Therefore, a task offloading strategy proposed by Yu *et al.* [23] is: For tasks with a large amount of data, the near-computing strategy should be used to save energy consumption caused by uploading tasks. For tasks with low computing power and less data, they can be uploaded to cloud computing to meet their computing power, and the energy paid by upload tasks is not much, so it can achieve better performance [23]. A task offloading scheme with load balancing proposed by Khafajiy *et al.* [24], where ESs of the Fog layer form a service group to provide services to the outside world. If an ES has a heavier load, it can also redistribute its own tasks to the lightly loaded ESs to achieve load balancing.

Resource allocation is also one of important research content. Generally, there may be multiple tasks that need to be executed on ESs [22], [25]. Executing tasks requires allocating computation resources such as CPU, memory, etc. Therefore, if more resources are allocated to a task, the time required to complete the task is smaller. However, since resources are limited and competitive, a good resource allocation can effectively improve resource utilization on the one hand, and shorten task processing time on the other hand. From the perspective of task scheduling, an ES is a resource body with multiple resources, so which ES to offload tasks belongs to a kind of resource scheduling with large granularity. From the perspective of fine-grained resource scheduling, Xu *et al.* [25] proposed a resource scheduling strategy based on matching theory. They believe that some tasks requiring more computing power should be allocated more CPU resources

while others tasks require more storage and communication resources. Thus, using matching theory to analyze computation resources in their method can achieve good results [25].

Thirdly, different transmission rates have an important impact on task completion. If a task is not offloaded, completion time is computation delay executed locally. If the task is offloaded, communication delay of task offloading to ESs will be increased. Therefore, if a communication way with high speed is selected, communication delay can be reduced [16]. However, the communication way is mostly determined by the hardware. For example, in the research of Liu *et al.* [16], the transmission speed using Vehicle to Infrastructure (V2I) is higher, so transmission rate is small. On the other hand, transmission rate is related to transmit power used during communication. Generally, if a larger transmit power is used, transmission rate is larger so that communication delay is smaller, but the communication-related energy consumption is usually increased [26]. Therefore, selection of transmit power becomes an important part of task offloading [26].

It is worth noting that although the above optimization methods and strategies have been more researched. However, the task offloading issue in this paper for IoTDs through MVs in IoV is more complicated than previous studies. The task offloading studied in this paper includes task transmission from IoTDs to MVs, and then MVs decide whether to offloading to ESs. Finally, after tasks are completed, the result need to be returned from MVs or ESs to IoTDs. Not only the task offloading path is long, but there are also optimization variables such as selection decisions, resource allocation, offloading ratio and transmit power. These optimization variables make task offloading need to meet task processing delay and resource constraints, so it is comparatively challenging.

III. SYSTEM MODEL AND DEFINITIONS

A. The vehicle-assisted VEC network

Considering a vehicle-assisted VEC network composed of a set of Road Side Units $\mathcal{M} = \{1, \dots, M\}$ and K Internet of Things (IoTs) denoted by $\mathcal{K} = \{1, \dots, K\}$ as shown in Fig. 1, where tasks can not only be computed locally, but also can be offloaded to vehicles for computing. Due to the limited computation resources, vehicles also act a relay to help computation bits of IoTDs transmit to RSUs equipped with a VEC server for offloading. Specifically, let ϱ_k ($0 \leq \varrho_k \leq 1$) be offloading ratio of the task from IoTD k , that is a ratio of the offloaded computation bits to the total computation bits. In the network, under different ϱ_k , there are three computation strategies: Strategy I: All computation bits of the task from IoTD k are computed locally; Strategy II: $(1 - \varrho_k)$ computation bits are computed locally while ϱ_k computation bits are offloaded to the vehicle; Strategy III: $(1 - \varrho_k)$ computation bits are computed locally while ϱ_k computation bits are offloaded to the server. Specifically (as shown in Fig. 1), when $\varrho_k = 0$, IoTD k only adopts Strategy I; when $0 < \varrho_k < 1$, IoTD k adopts the both Strategy I and Strategy II or the both Strategy I and Strategy III; when $\varrho_k = 1$, IoTD k adopts Strategy II or Strategy III: All computation bits of the task are offloaded to the vehicle or

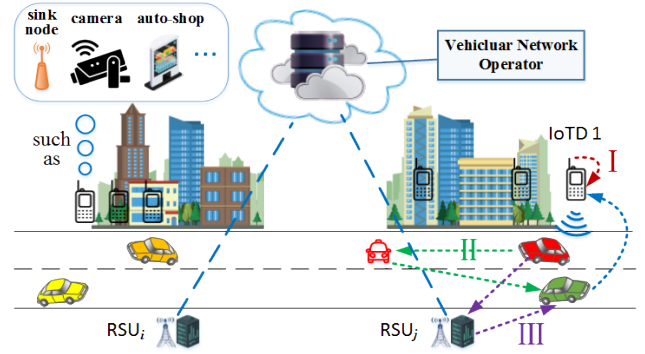


Fig. 1. The vehicle-assisted VEC network.

the server. Each IoTD generates a computation task in each time slot [27], such as numerical calculation, data analysis, image processing, etc. For convenience, we use sufficiently constant δ_t to divide the period T into N slots with equal size, which are given by a set $\mathcal{N} = \{1, \dots, N\}$. Specifically, the characteristics of a computation task can be represented by a 5-tuple parameter $u_k = \langle I_k, O_k, \tilde{c}_k, E_k^{max}, T_k^{max} \rangle$, $k \in \mathcal{K} = \{1, \dots, K\}$ where I_k and O_k indicate input and output data size of the task in terms of bits. \tilde{c}_k represents the required computation resources for completing the task. E_k^{max} and T_k^{max} stands for the maximum energy consumption and the maximum permissible latency for offloading the task u_k and returning a result, respectively. Vehicles running on the road collect tasks from nearby IoTDs. When a task is completed, its results are also returned to the corresponding IoTD via a vehicle. Note that, the vehicle does not need to follow a specific trajectory during the whole process. Ref. [12] summarized the probability that a taxi's random waypoint can cover the entire city area within half an hour and at least one taxi in each area within 10 minutes. And the taxis are only a small part of urban vehicles. Dynamics and randomness of vehicles make the vehicle-assisted VEC extremely complex. In order to simplify the progress, we assume that when a IoTD has a demand to upload a task or receive a result, there will always be vehicles passing the IoTD based on Ref. [12]. We will focus on dynamic arrival of vehicles in our future research work. Every IoTD, vehicle and VEC server is assumed equipped with one single antenna [27].

Considering that the life of IoTDs is constrained by energy and sensitive latency, each u_k can reach the vehicle via wireless channel for either computing or relaying. In particular, where tasks are offloaded is determined based on maximizing system utility. In other words, at the beginning of each time slot, Vehicular Network Operator (VNO) collects basic information about tasks from IoTDs. Meanwhile, the VNO also updates a resource allocation table (RAT) [28], the RAT records the available resources of each VEC server. Then the VNO determines a computation strategy for each IoTD by the proposed JOET algorithm. Specifically, if u_k is offloaded to the server, then computation resources allocated to u_k are more than resources provided by the vehicle to make up for the long-distance cost. The VEC servers all have the same initial resources $F[0]$. For RSU m , the free computation resources $F_m[n]$ at time slot n is equal to the sum of the remaining

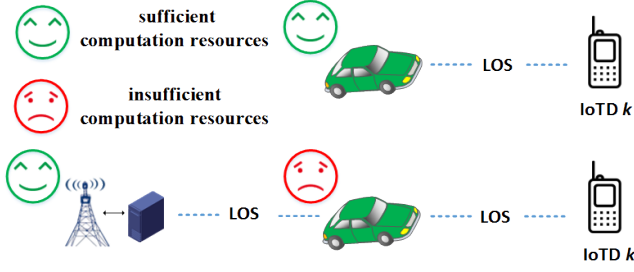


Fig. 2. Two typical scenarios I2V and I2V2S, which are explained in Section III-B1 and Section III-B2 respectively.

resources and the released resources at time slot $n - 1$.

B. Communication Model

1) *IoTD to Vehicle (I2V)*: For resources available at vehicles on the road, IoTD $k \in \mathcal{K}$ offloads a computation task to one of the passing vehicles. We define $x_k \in \{0, 1\}$ as a offloading decision variable, which indicates whether or not IoTD k offloads their computation bits to the vehicle via a wireless channel (as shown in Fig. 2). Note that, dynamics and randomness of vehicles make the vehicle-assisted VEC extremely complex, and we will focus on solving the characteristics in our future works. Thus, we consider vehicles to be static and do not number them. In other words, we consider that vehicles have the same functions and the same initial resources when computing tasks.

$$x_k = \begin{cases} 1, & \text{if } u_k \text{ is offloaded to the vehicle;} \\ 0, & \text{otherwise.} \end{cases} \quad (1)$$

Further, it is assumed that the wireless channel between IoTD k and vehicles is based on the line of sight (LOS) link [27], [29], hence the channels between IoTDs and vehicles are modeled by the free space path loss model. Therefore, channel power gain from IoTD k to the vehicle is given by:

$$h_{kv} = \beta_0 d_{kv}^{-2}, \quad (2)$$

where β_0 is channel gain at the reference distance $d_0 = 1\text{m}$, and d_{kv} indicates the distance between IoTD k and the vehicle collecting u_k . Similarly, $h_{vm} = \beta_0 d_{vm}^{-2}$ represents channel power gain from the vehicle to RSU m .

The total available bandwidth B is equally assigned to each IoTD. Define p_k as transmit power of u_k . Specifically, it is assumed that an OFDMA is applied in the system [27]. Thus, transmission rate in bits-per-second (b/s) from IoTD k to the vehicle collecting it for computing is defined as:

$$R_k^{k \rightarrow v} = B_k \log_2 \left(1 + \frac{p_v \xi_0}{d_{kv}^2} \right), \quad (3)$$

where $B_k = B/k$ and $\xi_0 = \frac{\beta_0}{N_0 B_k}$ is expressed as the reference received Signal-to-Noise Ratio (SNR) at IoTD k for $d_0 = 1\text{m}$ [27] transmission delay for dispatching a task from IoTD k to the vehicle is given by:

$$t_{k,c}^{k \rightarrow v} = \frac{\varrho_k I_k}{R_k^{k \rightarrow v}}. \quad (4)$$

Sometimes, we also face the return of computation results (or instructions). To solve the problem, our scheme considers

returning result and optimizes task processing delay. When u_k is completed by the vehicle collecting it, the vehicle delivers its results to the another vehicle passing through IoTD k (Strategy II in Fig. 1). Similarly, the wireless channel between the vehicles is based on the LOS link, but the channel B_k is unified as the channel accessed by vehicles participating in u_k . Note that, different from previous works [9], [27], [28], [30], We do not ignore results or set results of all tasks to a fixed smaller value for convenience. On the contrary, we integrate the returning results into task offloading by considering output data size to make it more complete. Further, given transmit power p_v of the vehicle, transmission rate in b/s from the transmitting vehicle to the receiving vehicle is defined as:

$$R_k^{v \rightarrow v} = B_k \log_2 \left(1 + \frac{p_v \xi_1}{d_{vv}^2} \right), \quad (5)$$

where d_{vv} is the distance from the transmitting vehicle to the receiving vehicle, which is equal to the distance traveled by the vehicle during computing the task, $\xi_1 = \frac{\beta_0}{N_1 B_k}$. In addition, $d_{vv} = \frac{\varrho_k \bar{c}_k \bar{v}}{F_v}$, where \bar{v} denotes the average speed of the vehicle. It can be observed from this formula that the returning time is related to the size of computation bits, so researching on the returning results is necessary. Besides, d_{vk} from the receiving vehicle to IoTD k is equal to d_{kv} from IoTD k to the vehicle collecting u_k , so that channel power gain h_{vk} from the vehicle to IoTD k is equal to h_{kv} . Thence, transmission rate in b/s is defined as:

$$R_k^{v \rightarrow k} = B_k \log_2 \left(1 + \frac{p_v \xi_1}{d_{kv}^2} \right). \quad (6)$$

In summary, transmission delay for returning results of u_k is given by:

$$t_{k,c}^{v \rightarrow k} = \frac{\varrho_k O_k}{R_k^{v \rightarrow v}} + \frac{\varrho_k O_k}{R_k^{v \rightarrow k}}. \quad (7)$$

Further, the communication-related delay for u_k is obtained as:

$$t_{k,c} = t_{k,c}^{k \rightarrow v} + t_{k,c}^{v \rightarrow k} = \frac{\varrho_k I_k}{R_k^{k \rightarrow v}} + \frac{\varrho_k O_k}{R_k^{v \rightarrow v}} + \frac{\varrho_k O_k}{R_k^{v \rightarrow k}}. \quad (8)$$

For IoTD k , energy consumption of uploading data from IoTD k to the vehicle is based on the classic transmission energy model [31], i.e., $E_k^{k \rightarrow v} = (p_k + p_k^{cir}) \cdot t_{k,c}^{k \rightarrow v}$, where p_k^{cir} is circuit power. Following a similar model in [32], p_k^{cir} can be calculated as $p_k^{cir} = \vartheta_k + (\frac{1}{\eta} - 1) \cdot p_k$, where ϑ_k is a transmission-power-independent component that takes possession of the power consumed by circuit, and η is power amplifier efficiency. The detailed parameters are summarized in TABLE I. Physically, η is defined by the drain efficiency of the RF power amplifier [33]. Thus, energy consumption of uploading data transmission at IoTD k can be rewritten as:

$$E_k^{k \rightarrow v} = \frac{1}{\eta} p_k t_{k,c}^{k \rightarrow v} + \vartheta_k t_{k,c}^{k \rightarrow v} = \frac{1}{\eta} (p_k + \vartheta_{k,c}) t_{k,c}^{k \rightarrow v}, \quad (9)$$

where $\vartheta_{k,c} = \eta \cdot \vartheta_k$ is defined as the equivalent circuit power consumption for data transmission. Energy consumption for receiving data is related to output data size of u_k [34]. For instance, if IoTD k receives O_k bits data, energy consumption is $E_k^{v \rightarrow k} = \varrho_k O_k e_c$, where e_c is a circuit power for receiving data. Note that, since energy consumption of task transmission

TABLE I: THE KEY NOTATION

Notation Definition	Notation (and Value)
Set of IoTs	$ \mathcal{K} = K = 40$
Set of VEC servers	$ \mathcal{M} = M = 6$
Task from IoTD k	u_k
Set of time slots	$ \mathcal{N} = N = 20$
Size of input data (bits)	I_k
Size of output data (bits)	O_k
Required resource for u_k	\tilde{c}_k
Offloading ratio of u_k	ϱ_k
Capacitance coefficient of u_k	$k_u = 10 \text{e-}27$
Maximum energy consumption	E_k^{max}
Maximum permissible latency	T_k^{max}
Total computation resources	F_k, F_V, F_m
Computation resources allocated at u_k at RSU m	f_{nm}
Decision variable	x_k, y_{km}
Channel gain at the reference distance	$\beta_0 = -50 \text{dB}$
$d_0 = 1 \text{ m}$	
Channel power gain	h_{kv}, h_{vm}
Maximum transmit power of each IoTD for offloading	$p_k^{max} = 30 \text{dBm}$
Maximum transmit power of vehicles and VEC servers for offloading	$p_v^{max} = p_m^{max} = 36 \text{dBm}$
Power amplifier efficiency	$\eta = 0.9$ [33]
Circuit power of IoTs	$\vartheta_{k,c} = 5 \text{mW}$
Communication bandwidth	$B = 120 \text{MHz}$
Energy consumption for receiving data	$e_c = 5 \text{nJ/bit}$
Transmission rate in b/s	$R_k^{k \rightarrow v}, R_k^{v \rightarrow v}, \dots$
Transmission delay	$t_{k,c}^{k \rightarrow v}, t_{k,c}^{v \rightarrow v}, \dots$
Excution delay	$t_{k,e}^{loc}, t_{k,e}^{veh}, \dots$
Noise power spectrum density	$N_0 = N_1 = N_2 = -130 \text{dBm/Hz}$
Reference received signal-to-noise ratio (SNR)	ξ_0, ξ_1, ξ_2

and computation is negligible for the vehicle, we do not consider reducing energy consumption by optimizing transmit power of the vehicle.

In our model, the total communication-related energy consumption for u_k in a time slot is denoted as:

$$E_k^{com} = \frac{1}{\eta} (p_k + \vartheta_{k,c}) \cdot \frac{\varrho_k I_k}{R_k^{k \rightarrow v}} + \varrho_k O_k e_c. \quad (10)$$

Further, the constraint on p_k is defined as follows:

$$0 < p_k < p_k^{max}, \forall k \in \mathcal{K}, \quad (11)$$

where p_k^{max} is the maximum transmit power of IoTD k . For convenience, we assume that each IoTD has enough energy in each time slot to transmit their task and receive the related result. In the next research work, we will focus on the random energy harvesting process.

2) *IoTD to Vehicle to Server (I2V2S)*: When u_k is required to be dispatched to the VEC server, the VNO also determine the server's selection decisions for u_k according to JOET and then informs the vehicle collecting u_k the decision. Moreover, we assume that VEC servers belong to the same VNO, where

RAT keeps the track of the available resources of VEC servers. Then, the vehicle offloads the collected task to the target server, and the wireless channel is also based on LOS link. We denote $y_k^{k \rightarrow m}$ as a decision variable, which indicates whether or not u_k is offloaded from the vehicle collecting it to RSU m , which is given by:

$$y_k^{k \rightarrow m} = \begin{cases} 1, & \text{if } u_k \text{ is offloaded to RSU } m; \\ 0, & \text{otherwise.} \end{cases} \quad (12)$$

Similarly, transmission rate $R_k^{v \rightarrow m}$ from the vehicle collecting u_k to RSU m is given by:

$$R_k^{v \rightarrow m} = B_k \log_2 \left(1 + \frac{p_v \xi_2}{d_{vm}^2} \right), \quad (13)$$

where $\xi_2 = \frac{\beta_0}{N_2 B_k}$, d_{vm} is the distance from the vehicle to RSU m . Transmission delay for dispatching a task from IoTD k to RSU m is expressed as:

$$t_{k,c}^{k \rightarrow m} = t_{k,c}^{k \rightarrow v} + t_{k,c}^{v \rightarrow m} = \frac{\varrho_k I_k}{R_k^{k \rightarrow v}} + \frac{\varrho_k I_k}{R_k^{v \rightarrow m}}. \quad (14)$$

Analogously, when RSU m completed u_k , RSU m delivers its results to the vehicle passing though IoTD k , and then the vehicle delivers the results to IoTD k . Given transmit power p_m of RSU m , transmission rate from RSU m to the vehicle receiving the results is denoted as:

$$R_k^{m \rightarrow v} = B_k \log_2 \left(1 + \frac{p_m \xi_2}{d_{mv}^2} \right), \quad (15)$$

where d_{mv} is the distance from RSU m the vehicle receiving the results. Transmission delay for returning the results from RSU m to IoTD k is given by:

$$t_{k,c}^{m \rightarrow k} = t_{k,c}^{m \rightarrow v} + t_{k,c}^{v \rightarrow k} = \frac{\varrho_k O_k}{R_k^{m \rightarrow v}} + \frac{\varrho_k O_k}{R_k^{v \rightarrow k}}. \quad (16)$$

Although u_k is transmitted to RSU m for offloading through the vehicle, for IoTD k , the total communication-related energy consumption is still E_k^{com} .

C. Computation Model

1) *Computation at Vehicle*: Considering the sensitive delay and the life limited by energy consumption, IoTD k computes $(1 - \varrho_k) \tilde{c}_k$ locally, and offloads the rest $\varrho_k \tilde{c}_k$ to the vehicle and the VEC server. The initial free resources of all vehicles are given by F_V . Since computation resources of vehicles are insufficient, we consider that each vehicle can only compute one task. In other words, the vehicle collecting u_k allocates all resources to u_k . Thus, computation delay for u_k at the vehicle is denoted as:

$$t_{k,e}^{k \rightarrow v} = \frac{\varrho_k \tilde{c}_k}{F_V}. \quad (17)$$

Besides, the local computation time $t_{k,e}^{loc}$ can be given by:

$$t_{k,e}^{loc} = \frac{(1 - \varrho_k) \tilde{c}_k}{F_k}, \quad (18)$$

where F_k is the total resources of u_k . Referring to Ref. [35], the computation-related energy consumption is expressed as:

$$E_k^{exe} = k_u F_k^2 (1 - \varrho_k) \tilde{c}_k, \quad (19)$$

where $k_u F_k^2$ is the power consumption per CPU cycle and k_u denotes capacitance coefficient that depends on chip architecture [36]. Thus, the total energy consumption is denoted as $E_k = E_k^{com} + E_k^{exe}$. Further, when u_k is offloaded to the vehicle, task processing delay is determined by:

$$t_k^{k \rightarrow v} = \max \{ t_{k,e}^{loc}, t_{k,c}^{k \rightarrow v} + t_{k,e}^{veh} + t_{k,c}^{v \rightarrow v} + t_{k,c}^{v \rightarrow k} \}. \quad (20)$$

2) *Computation at VEC Server*: Sometimes, u_k is dispatched to the VEC server to achieve greater system utility because the vehicle does not have enough computation resources. The VNO derives selection decisions, resource allocation, offloading ratio and transmit power for each IoTD k based on the proposed JOET algorithm. We denote $f_{km} \leq F_m$ as computation resources allocated to u_k at RSU m , where F_m as the total computation resources of RSU m . While minimizing the task processing delay and the energy consumption of IoTDs, we also considered how to optimize load balancing of servers. Therefore, execution delay for u_k at RSU m is obtained as:

$$t_{k,e}^{k \rightarrow m} = \frac{\varrho_k \tilde{C}_k}{f_{km}}. \quad (21)$$

For u_k offloaded to RSU m , task processing delay is expressed as:

$$t_k^{k \rightarrow m} = \max \{ t_{k,e}^{loc}, t_{k,c}^{k \rightarrow m} + t_{k,e}^{ser} + t_{k,c}^{m \rightarrow k} \}. \quad (22)$$

In summary, task processing delay T_k is given by:

$$T_k = x_k t_k^{k \rightarrow v} + (1 - x_k) \sum_{m \in \mathcal{M}} y_{km} t_k^{k \rightarrow m}. \quad (23)$$

D. Problem formulation

According to the above discussion, our objective is to optimize jointly the total energy consumption and task processing delay in consideration of load balancing. We formulate the objective problem as a system utility maximization problem, which is subjected to selection decisions, resource allocation, offloading ratio and transmission power adjustment. Specifically, the utility function is defined as:

$$\sum_{n \in \mathcal{N}} U[n] \triangleq \sum_{n \in \mathcal{N}} \sum_{k \in \mathcal{K}} \log \left(1 + \alpha \frac{E_k^{max}[n] - E_k[n]}{E_k^{max}[n]} + \beta \frac{T_k^{max}[n] - T_k[n]}{T_k^{max}[n]} \right). \quad (24)$$

where α and β are the weight of each items respectively, indicating importance of each item. $E_k^{max}[n]$ and $T_k^{max}[n]$ are the maximum energy consumption and the maximum task processing delay for u_k in time slot n . The utility function as a satisfaction function monotonically decreases with E_k and T_k . In other words, we minimize E_k and T_k to maximize system utility in each time slot. The logarithmic utility is known as proportional fairness based on [37], [38] which is able to achieve load balancing [38]. Therefore, we formulate the utility maximization problem as:

$$\begin{aligned} P1: \quad & \max_{\mathbf{x}, \mathbf{y}, \mathbf{F}, \boldsymbol{\varrho}, \mathbf{P}} \\ & \text{s.t. (1), (11) and (12);} \\ & x_k t_k^{k \rightarrow v} \leq T_k^{max}, \forall k \in \mathcal{K}; \end{aligned} \quad (25a)$$

$$\sum_{m \in \mathcal{M}} y_{km} [x_k t_k^{k \rightarrow v} + (1 - x_k) t_k^{k \rightarrow m}] \leq T_k^{max}, \forall k \in \mathcal{K}; \quad (25b)$$

$$\sum_{m \in \mathcal{M}} y_{km} = 1, \forall k \in \mathcal{K}; \quad (25c)$$

$$0 \leq \sum_{k \in \mathcal{K}} y_{km} f_{km} \leq F_m, \forall m \in \mathcal{M}; \quad (25d)$$

$$0 \leq \sum_{m \in \mathcal{M}} y_{km} \varrho_k \leq 1, \forall k \in \mathcal{K}; \quad (25e)$$

$$0 \leq \varrho_k \leq 1, \forall k \in \mathcal{K}, \quad (25f)$$

where constraints (25a) and (25b) guarantee that task processing delay cannot exceed the maximum permission delay T_k^{max} , and constraint (25c) are used to ensure that u_k can only be computed by one server. Constraint (25d) means that the sum of allocated resources to tasks which select RSU m does not exceed F_m . Specifically, the lower bound of p_k is also constrained in constraints (25a) and (25b). Constraints (25e) and (25f) denote offloading ratio of u_k cannot exceed to 1. In addition, as mentioned earlier, u_k 's allocated resources are $F_V < f_{km}$ when u_k is offloaded to the vehicle. This is because f_{km} needs to make up for transmission time from the vehicle to the server.

Our objective is to optimize jointly the total energy consumption and task processing delay under the premise of ensuring that the task is completed. Similar to Ref. [30], due to the integer constraint y_{km} , P1 is a mixed integer nonlinear programming problem. But the problem to be solved in this paper is more difficult than Ref. [30] because we not only need to optimize task processing delay, but also the total energy consumption. In the following section, we will pour attention to how to solve this more intractable problem.

IV. PROBLEM DECOMPOSITION AND SOLUTION

Since there are highly complex coupling among optimization variables and mixed combinatorial feature in P1, it is quite challenging to solve P1. Let a binary matrix $\mathbf{x} = \{x_k | \forall k \in \mathcal{K}\}$, a binary matrix $\mathbf{y} = \{y_{km} | \forall k \in \mathcal{K}, m \in \mathcal{M}\}$, a matrix $\mathbf{F} = \{f_{km} | \forall k \in \mathcal{K}, m \in \mathcal{M}\}$, a matrix $\boldsymbol{\varrho} = \{\varrho_k | \forall k \in \mathcal{K}\}$ and a matrix $\mathbf{P} = \{p_k | \forall k \in \mathcal{K}\}$, denote offloading decision, server selection decision, resource allocation, offloading ratio and transmit power, respectively. In this section, we aim to decouple \mathbf{x} and \mathbf{y} , \mathbf{F} , $\boldsymbol{\varrho}$ and \mathbf{P} into two subproblems (i.e., optimization of selection decisions, optimization of resource allocation, offloading ratio and transmit power). That is, we firstly determine \mathbf{x} and \mathbf{y} under given \mathbf{F} , $\boldsymbol{\varrho}$ and \mathbf{P} , and then \mathbf{F} , $\boldsymbol{\varrho}$ and \mathbf{P} under obtained \mathbf{x} and \mathbf{y} , and repeat this process until convergence.

To facilitate the introduction of JOET, we define the following intermediate variables:

$$\begin{cases} a_{km} = \frac{E_k^{max} - E_k^{com}}{E_k^{max}}; \\ b_{km} = \frac{T_k^{max} - T_k^{pro}}{T_k^{max}}. \end{cases} \quad (26)$$

Therefore, taking time slot n as an example, the utility function can be rewritten as:

$$U[n] \triangleq \sum_{k \in \mathcal{K}} \log(1 + \alpha a_{km} + \beta b_{km}). \quad (27)$$

A. Optimization of Selection Decisions

The selection decisions problem under given \mathbf{F} , $\boldsymbol{\rho}$ and \mathbf{P} can be formulated as:

$$\begin{aligned} P1.1: \quad & \max_{\mathbf{x}, \mathbf{y}} U \\ & \text{s.t. (1), (12), (25a), (25b) and (25c)}. \end{aligned} \quad (28)$$

Since all the indicator variables \mathbf{x} and \mathbf{y} are binary and the objective function is nonlinear with respect to \mathbf{x} and \mathbf{y} , $P1.1$ is also a MINLP problem [30], [39]. Thus, we cannot obtain the optimal \mathbf{x} and \mathbf{y} in polynomial time. To solve it with low complexity, we employ an approximation algorithm, which firstly relaxes $P1.1$ as a continuous nonlinear programming problem and uses the Block Successive Upper-bound Minimization (BSUM) method to solve it.

To better describe optimization of selection decisions, we briefly introduce BSUM. The advantages of BSUM reside in both solution speed and problem decomposability [28], [40]. The standard form of BSUM is:

$$\begin{aligned} & \min_{\mathbf{z}} g(\mathbf{z}_1, \mathbf{z}_2, \dots, \mathbf{z}_J), \\ & \text{s.t. } \mathbf{z}_j \in \mathcal{Z}_j, \forall j \in \mathcal{J}, j = 1, \dots, J, \end{aligned} \quad (29)$$

where $\mathcal{Z} := \mathcal{Z}_1 \times \dots \times \mathcal{Z}_J$, $g(\cdot)$ is a continuous function and I is the set of indexes. For $j = 1, \dots, J$, we consider \mathcal{Z}_j as a closed convex set and \mathbf{z}_j as a block of variables. Similar to Block Coordinate Descent (BCD), at each iteration i , a single block of variables is optimized by solving the following problem:

$$\mathbf{z}_j^i \in \underset{\mathbf{z}_j \in \mathcal{Z}_j}{\operatorname{argmin}} g(\mathbf{z}_j, \mathbf{z}_{-j}^{i-1}), \quad (30)$$

where $\mathbf{z}_{-j}^{i-1} := (\mathbf{z}_1^{i-1}, \dots, \mathbf{z}_{j-1}^{i-1}, \mathbf{z}_{j+1}^{i-1}, \dots, \mathbf{z}_J^{i-1})$, $\mathbf{z}_l^i = \mathbf{z}_l^{i-1}$ for $j \neq l$. Since \mathbf{x} and \mathbf{y} are integer variables, $P1.1$ is a non-convex function to make the problem more difficult, and BCD does not always guarantee convergence. BSUM is an improved method of BCD. More details are presented in Ref. [28] and Ref. [40].

Thus, we consider BSUM as a suitable candidate method for solving it by focusing on solving perblock problems. Using BSUM to solve $P1.1$, we need two steps:

- i) Step 1: we introduce a proximal function which is a convex optimization problem and an upper bound of $P1.1$ by adding quadratic penalization [28];
- ii) Step 2: By negating the system utility function to turn it into a minimization problem as $B(x, y) := -U$. Then we minimize the proximal upper-bound function and ensure that the upper-bound function takes steps proportional to the negative value of gradient.

At each iteration i , $\forall j \in \mathcal{J}$, we define the proximal upper-bound function B_j , which is convex and the proximal upper-bound of the objective function defined in (28). To make B_j convex, we introduction a quadratic penalization, as follows:

$$\begin{aligned} B_j(\mathbf{z}_j, \mathbf{x}^{(i)}, \mathbf{y}^{(i)}) & := B(\mathbf{z}_j, \mathbf{x}^{(i-1)}, \mathbf{y}^{(i-1)}) \\ & \quad + \frac{\delta_j}{2} \|\mathbf{z}_j - \mathbf{x}^{(i-1)}\|^2. \end{aligned} \quad (31)$$

Herein, (31) is the proximal upper-bound of (28) and it also can be employed to other vector of variable \mathbf{y} . where $\delta_j > 0$ indicates the positive penalty parameter. Further, eq. (31) is a convex optimization problem because of its quadratic term $\frac{\delta_j}{2} \|\mathbf{z}_j - \mathbf{x}^{(i-1)}\|^2$, where $\mathbf{x}^{(i-1)}$ and $\mathbf{y}^{(i-1)}$ are considered to be the solution of the previous step ($i-1$). Next, we update the solution by the following formula:

$$\mathbf{x}^{(i+1)} \in \min_{\mathbf{x}} B_j(\mathbf{x}^{(i+1)}, \mathbf{x}^{(i)}, \mathbf{y}^{(i)}), \quad (32)$$

$$\mathbf{y}^{(i+1)} \in \min_{\mathbf{y}} B_j(\mathbf{y}^{(i+1)}, \mathbf{x}^{(i)}, \mathbf{y}^{(i)}). \quad (33)$$

We adopt the BSUM method of Ref. [40] to solve (32) and (33). The solution process is presented in the following Algorithm 1 (BSUM for Optimization of Selection Decisions), which is consistent with BSUM in Ref. [40]. Herein, we employ the Cyclic rule to select each coordinate $j \in \mathcal{J}$ [40]. This is because a task is transmitted to the vehicle first, and only when the vehicle cannot meet the maximum delay of the task or achieve a lower system benefit, the task will be offloaded to the server.

Algorithm 1 BSUM for Optimization of Selection Decisions

Input: \mathbf{x} and \mathbf{y}

Output: \mathbf{x}^* and \mathbf{y}^*

- 1: Initialize $i = 0, \epsilon > 0$;
 - 2: Find initial feasible points ($\mathbf{x}^{(0)}, \mathbf{y}^{(0)}$)
 - 3: **repeat**
 - 4: Choose index set I by Cyclic rule, i.e., $1, 2, 1, \dots$;
 - 5: Relax \mathbf{x} , and let $\mathbf{x}^{(i+1)} \in \min_{\mathbf{x}} B_j(\mathbf{x}^{(i+1)}, \mathbf{x}^{(i)}, \mathbf{y}^{(i)})$;
 - 6: Set $x_k^{(i+1)} = x_k^{(i)}, \forall k \notin \mathcal{J}$;
 - 7: **if** $x_k^{(i)} \geq \rho$ **then**
 - 8: $x_k^{(i+1)} = 1$;
 - 9: **else**
 - 10: $x_k^{(i+1)} = 0$;
 - 11: **end if**
 - 12: Jump to step 4, obtain $\mathbf{y}^{(i+1)}$ by solving (33);
 - 13: $i = i + 1$
 - 14: **until** $\| \frac{B_j^{(i)} - B_j^{(i+1)}}{B_j^{(i)}} \| \leq \epsilon$
 - 15: **Then**, consider $\mathbf{x}^* = \mathbf{x}^{(i+1)}, \mathbf{y}^* = \mathbf{y}^{(i+1)}$;
-

Algorithm 1 (BSUM for Optimization of Selection Decisions) can be considered as a generalized form of BCD, which optimizes the upper-bound function of the original objective function block by block. In Algorithm 1, we determine the offloading decision x_k for each u_k by first relaxing x_k and then (32). Note that, relaxing details will be introduced below, and we first introduce the complete structure of Algorithm 1. If $x_k = 1$, the user transmit its task to a passing vehicle; else, u_k will be computed locally. Similar to x , we further determine the server selection y_{km} for each u_k . If $y_{km} = 1$, then u_k will

be offload to RSU m ; else, u_k will be computed the vehicle. At each iteration $i+1$, we update the solution by solving (32) and (33) until $\| \frac{B_j^{(i)} - B_j^{(i+1)}}{B_j^{(i)}} \| \leq \epsilon$, where $\epsilon \in (0, 1)$.

When Algorithm 1 is used to solve (32) and (33), we first relax the vectors of variables \mathbf{x} and \mathbf{y} into a continuous value in $[0, 1]$, and then we use a threshold rounding method [41] to compel the relaxed \mathbf{x} and \mathbf{y} to be vectors of binary variables.

Taking \mathbf{x} as an example, we set the feasible solution $x_k^{i*} \in \mathbf{x}^i$ as follows:

$$x_k^{i*} = \begin{cases} 1, & \text{if } x_k^{i*} \geq \rho; \\ 0, & \text{otherwise.} \end{cases} \quad (34)$$

where $\rho \in (0, 1)$ is a positive rounding threshold. The above round method can also be used to \mathbf{y} . However, the obtained binary solution may break communication and computational constraints (25a) and (25b). To avoid this issue after rounding, we solve (31) in the form of $B_j + \varepsilon\Delta$, where ε is a constant weight. Then, constraints are modified as follows:

$$x_k t_k^{k \rightarrow v} \leq T_k^{max} + \Delta_x, \quad \forall k \in \mathcal{K}; \quad (35)$$

$$\sum_{m \in \mathcal{M}} y_{km} t_k^{k \rightarrow m} \leq T_k^{max} + \Delta_y, \quad \forall k \in \mathcal{K}, \quad (36)$$

where Δ_x and Δ_y are the maximum break of communication and computation resources, $\Delta = \Delta_x + \Delta_y$. Unlike Ref. [28], we integrate communication and computation resources into task processing time to minimize the time. Δ_x and Δ_y are given by:

$$\Delta_x = \max \{0, x_k t_k^{k \rightarrow v} - T_k^{max}\}, \quad \forall k \in \mathcal{K}; \quad (37)$$

$$\Delta_y = \max \{0, \sum_{m \in \mathcal{M}} y_{km} t_k^{k \rightarrow m} - T_k^{max}\}, \quad \forall k \in \mathcal{K}. \quad (38)$$

If Δ_x and Δ_y , we didn't break constraints (25a) and (25b). Next, we take the integrality gap to measure the ratio between the feasible solutions of B_j and $B_j + \varepsilon\Delta$. According to definition and proof of integrality gap in Ref. [40], we can copy the following definition:

Definition 1 (Integrality gap). Given problem (31) and its rounded problem $B_j + \varepsilon\Delta$, the integrality gap is given by:

$$\vartheta = \min_{\mathbf{x}, \mathbf{y}} \frac{B_j}{B_j + \varepsilon\Delta}. \quad (39)$$

We obtain B_j through relaxation of variables \mathbf{x} and \mathbf{y} while we get $B_j + \varepsilon\Delta$ after rounding the relaxed $\mathbf{x}^{(i)}$ and $\mathbf{y}^{(i)}$. Then, when ϑ ($\vartheta \leq 1$) is close to 1 [40], we achieve the best rounding. That is if $\vartheta = 1$, then $\Delta_x = 0$ and $\Delta_y = 0$.

Further, according to Ref. [40] and Ref. [28], we have the following remark:

Remark 1 (Convergence). BSUM for optimization of selection decisions takes $\mathcal{O}(\log(1/\epsilon))$ to converge to an ϵ -optimal solution.

According to Section II-D of Ref. [40], BSUM takes at most c/ϵ iterations to find an ϵ -optimal solution, where $c > 0$ is a constant only related to the description of a problem. Further, for different special forms of BSUM, the constant c in front of $1/\epsilon$ can be significantly refined so that it is independent of problem dimension [14], [40]. So BSUM takes $\mathcal{O} \log(1/\epsilon)$ to coverage to an ϵ -optimal solution.

B. Joint Optimization of Resource Allocation, Offloading Ratio and Transmit Power

Given selection decisions combination vectors \mathbf{z} , P1 is a joint optimization of resource allocation, offloading ratio and transmit power problem, which is formulated as:

1) *Computation at Vehicle:* Unlike the server, since the vehicle can only compute one task at a time and do its best to complete it, we just need to optimize offloading ratio and transmit power of u_k . However, according to (20), $t_k^{k \rightarrow v}$ is nondifferentiable with respect to ϱ_k and p_k . To solve this problem, we do the following approximate:

$$P1.2 : \max_{\mathbf{F}, \varrho, \mathbf{P}} U$$

$$\text{s.t. (11), (25a), (25b), (25d), (25e) and (25f)}. \quad (40)$$

Since the resource allocation constraints on the vehicle and the server are different, we solve them separately for above two case.

$$\begin{aligned} t_k^{k \rightarrow v} &\leq \frac{(1 - \varrho_k) \tilde{c}_k}{F_k} + \frac{\varrho_k I_k}{R_k^{k \rightarrow v}} + \frac{\varrho_k \tilde{c}_k}{F_V} + \frac{\varrho_k O_k}{R_k^{v \rightarrow v}} + \frac{\varrho_k O_k}{R_k^{v \rightarrow k}} \\ &= \varrho_k r_{kv} + \frac{\varrho_k O_k}{R_k^{v \rightarrow v}} + \frac{\tilde{c}_k}{F_k}, \end{aligned} \quad (41)$$

where $r_{kv} = \frac{I_k}{R_k^{k \rightarrow v}} + \frac{(F_k - F_V) \tilde{c}_k}{F_k F_V} + \frac{O_k}{R_k^{v \rightarrow k}}$. From (35), we can obtain that the upper-bound of $t_k^{k \rightarrow v}$ is $\varrho_k r_{kv} + O_k / R_k^{v \rightarrow v} + \tilde{c}_k / F_k$. Further, we first rewrite P1.2 under the worst case delay. Thus, P1.2 is transformed into P1.2.1.

$$P1.2.1 : \max_{\varrho, \mathbf{P}} U$$

$$\text{s.t. (11), (25a), (25e) and (25f)}. \quad (42)$$

Furthermore, according to Lemma 1, P1.2.1 is a nonconvex optimization problem. Moreover, offloading ratio and transmit power are coupled with each other in both the objective function and constraints. Thus, we have developed a low-complexity algorithm by decoupling two variables. In other words, we derive ϱ under given \mathbf{P} and then derive \mathbf{P} under given ϱ and repeat this process until convergence.

Lemma 1: P1.2.1 is a nonconvex problem.

Proof: See the Appendix A. □

(1) *Offloading Ratio:* Under given \mathbf{P} , we can rewritten P1.2.1 as the offloading ratio adjustment problem as follows:

$$\begin{aligned} P1.2.1.1 : \max_{\varrho} \log \left(1 + \alpha a_{k0} + \beta \frac{T_k^{max} - t_k^{k \rightarrow v}}{T_k^{max}} \right) \\ \text{s.t. (25a), (25e) and (25f)}. \end{aligned} \quad (43)$$

Since $\partial^2 U / \partial \varrho^2 \leq 0$ based on Lemma 1, P1.2.1.1 is convex combining with linear constraint ϱ_k . In addition, under given \mathbf{F} and \mathbf{P} , ϱ are independent of each other. Thus, we apply primal-dual Lagrangian method to solve this problem. The Lagrangian function is constructed as follows:

$$\begin{aligned} \mathcal{L}(\varrho, \zeta, \varsigma, \tau) &= \sum_{k \in \mathcal{K}} \log \left(1 + \alpha a_{k0} + \beta \frac{T_k^{max} - t_k^{k \rightarrow v}}{T_k^{max}} \right) - \\ &\zeta_k \left(\varrho_k r_{kv} + \frac{\varrho_k O_k}{R_k^{v \rightarrow v}} + \frac{\tilde{c}_k}{F_k} - T_k^{max} \right) - \varsigma_k (\varrho_k - 1) + \tau_k \varrho_k, \end{aligned} \quad (44)$$

where ζ_k, ς_k and τ_k are the Lagrangian multipliers. Since ϱ_k is independent, the following complementary Slackness conditions must be satisfied based on the KKT conditions [42]:

$$\begin{aligned} \zeta_k \left(\varrho_k r_{kv} + \frac{\varrho_k O_k}{R_k^{v \rightarrow v}} + \frac{\tilde{c}_k}{F_k} - T_k^{max} \right) &= 0; \\ 0 &\leq \varrho_k \leq 1; \\ \varsigma_k (\varrho_k - 1) &= 0; \\ \tau_k \varrho_k &= 0; \\ \gamma_k > 0, \phi_k \geq 0, \psi_k \geq 0. \end{aligned} \quad (45)$$

Further, the first derivative of ϱ_k can be obtained as follows:

$$\begin{aligned} \frac{\partial \mathcal{L}(\varrho, \zeta, \varsigma, \tau)}{\partial \varrho} &= -\frac{1}{\ln(2)} \frac{I_k \omega_1 / R_k^{k \rightarrow v} + \omega_2 + \omega_3}{\omega_0} \\ &\quad - \zeta_k (r_{kv} + \omega_3) - \varsigma_k + \tau_k, \end{aligned} \quad (46)$$

where $\omega_0 = 1 + \alpha a_{k0} + \beta b_{k0}$, $\omega_1 = \frac{\alpha(p_k + \vartheta_{k,c})}{\eta E_k^{max}} + \frac{\beta}{T_k^{max}}$, $\omega_2 = \frac{\beta}{T_k^{max}} \left(\frac{(F_k - F_V) \tilde{c}_k}{F_k F_V} + \frac{O_k}{R_k^{v \rightarrow k}} \right) + \frac{\alpha(O_k e_c - k_u F_k^2 \tilde{c}_k)}{E_k^{max}}$ and $\omega_3 = \frac{O_k}{R_k^{v \rightarrow v}} + \frac{\varrho_k \tilde{c}_k \bar{v}}{d_{vv}^3 F_V} \times \frac{2B_k O_k p_v \xi_1}{\ln(2) (R_k^{v \rightarrow v})^2 (1 + \frac{p_v \xi_1}{d_{vv}^2})}$.

By taking $\partial \mathcal{L}(\varrho, \zeta, \varsigma, \tau) / \partial \varrho = 0$, ϱ^* can be obtained. However, considering the slackness condition of $\varsigma_k (\varrho_k - 1) = 0$ and $\tau_k \varrho_k = 0$, we face the following four possible cases:

Case 1: $\varsigma_k > 0$ and $\tau_k = 0$. Then, $\varrho_k = 1$. It means that the whole computation bits of u_k is offloaded to the vehicle;

Case 2: $\varsigma_k = 0$ and $\tau_k > 0$. Then, $\varrho_k = 0$. It means that u_k is computed locally.

Case 3: $\varsigma_k > 0$ and $\tau_k > 0$. In the case, there is not ϱ_k satisfying all KTT conditions.

Case 4: $\varsigma_k = 0$ and $\tau_k = 0$. Then, $\zeta_k (\varrho_k r_{kv} + O_k / R_k^{v \rightarrow v} + \tilde{c}_k / F_k - T_k^{max}) = 0$ and $\partial \mathcal{L}(\varrho, \zeta, \varsigma, \tau) / \partial \varrho = 0$. Due to $d_{vv} = \varrho_k \tilde{c}_k \bar{v} / F_V$, the approximate optimal ϱ^* can be obtained by iteration methods of nonlinear equations [43]. Therefore,

$$\begin{aligned} \zeta_k &= -\frac{1}{\ln(2)} \frac{I_k \omega_1 / R_k^{k \rightarrow v} + \omega_2 + \omega_3}{\omega_0 (r_{kv} + \omega_3)}; \\ \varrho_k &= \varrho_k^{j*}, \end{aligned} \quad (47)$$

where ϱ_k^{j*} and denotes that ϱ_k reaches convergence at the j th iteration. According to above analysis, we obtain the solution ϱ_k as:

$$\varrho_k = \begin{cases} \varrho_k^{j*}, & \text{if } \varsigma_k = 0 \text{ and } \tau_k = 0; \\ 1, & \text{if } \varsigma_k > 0 \text{ and } \tau_k = 0; \\ 0, & \text{if } \varsigma_k = 0 \text{ and } \tau_k > 0. \end{cases} \quad (48)$$

(2) *Transmit Power*: Further, P1.2.1 is transformed into P1.2.1.2 under given ϱ .

$$\begin{aligned} P1.2.1.1: \quad &\max_{\mathbf{P}} \log(1 + \alpha a_{k0} + \beta b_{k0}) \\ \text{s.t. (11) and (25a).} \end{aligned} \quad (49)$$

Similarly, $\partial^2 U / \partial \mathbf{P}^2 \leq 0$ based on Lemma 1. Combining with the linear constraint p_k , P1.2.1.2 is also a convex optimization problem. The process of solving this problem is the same as that of P1.2.1.1. Due to limited space of this

paper, we will not repeat it here. Referring to P1.2.1.1, the optimal solution of p_k is obtained as:

$$p_k^* = \begin{cases} \frac{d_{kv}^2}{\xi_0} (2^{\frac{\varrho_k I_k}{\Omega_k B_0}} - 1), & \text{if } \phi_k = 0 \text{ and } \psi_k = 0; \\ \xi_0, & \text{if } \phi_k > 0 \text{ and } \psi_k = 0, \end{cases} \quad (50)$$

where $\Omega_k = T_k^{max} - \frac{\varrho_k O_k}{R_k^{v \rightarrow v}} - \frac{\tilde{c}_k}{F_k} - \frac{\varrho_k O_k}{R_k^{v \rightarrow k}} - \frac{(F_k - F_V) \varrho_k \tilde{c}_k}{F_k F_V}$.

2) *Computation at VEC Server*: On the contrary, when the task is offloaded to the server, we not only need to sustainably reduce energy consumption and task processing delay of u_k , but also need to balance the load of servers by optimizing the allocation of computation resources. Similarly, according to (22), $t_k^{k \rightarrow m}$ is nondifferentiable with respect to ϱ_k and p_k . Thus, we again approximate $t_k^{k \rightarrow m}$ as follows:

$$\begin{aligned} t_k^{k \rightarrow m} &\leq \frac{(1 - \varrho_k) \tilde{c}_k}{F_k} + \frac{\varrho_k I_k}{R_k^{k \rightarrow v}} + \frac{\varrho_k I_k}{R_k^{v \rightarrow m}} + \frac{\varrho_k \tilde{c}_k}{f_{km}} + \frac{\varrho_k O_k}{R_k^{m \rightarrow v}} \\ &\quad + \frac{\varrho_k O_k}{R_k^{v \rightarrow k}} = \varrho_k r_{km} + \frac{\tilde{c}_k}{F_k}, \end{aligned} \quad (51)$$

where $r_{km} = \frac{I_k}{R_k^{k \rightarrow v}} + \frac{I_k}{R_k^{v \rightarrow m}} + \frac{(F_k - f_{km}) \tilde{c}_k}{F_k f_{km}} + \frac{O_k}{R_k^{m \rightarrow v}} + \frac{O_k}{R_k^{v \rightarrow k}}$. Similarly, $\varrho_k r_{km} + \tilde{c}_k / F_k$ is the upper bound of $t_k^{k \rightarrow m}$. P1.2 is transformed into P1.2.2 under the worst case delay.

$$\begin{aligned} P1.2.2: \quad &\max_{\mathbf{F}, \varrho, \mathbf{P}} U \\ \text{s.t. (11), (25b), (25d), (25e) and (25f).} \end{aligned} \quad (52)$$

Lemma 2: P1.2.2 is a nonconvex problem.

Proof: See Appendix B on the appendix file. \square

According to Lemma 2, P1.2.2 is also a nonconvex problem. In addition, \mathbf{F}, ϱ and \mathbf{P} are highly coupled with each other. Therefore, we further decouple three variables to develop a low-complexity method. Specifically, we derive \mathbf{F} under given ϱ and \mathbf{P} and then derive ϱ and \mathbf{P} under given \mathbf{F} , and repeat this process until convergence.

(1) *Computation Resources*: Under given ϱ and \mathbf{P} , we can rewrite P1.2.2 as the computation resource allocation problem P1.2.2.1 as:

$$\begin{aligned} P1.2.2.1: \quad &\max_{\mathbf{F}} U \\ \text{s.t. (25b) and (25d).} \end{aligned} \quad (53)$$

Since f_{km} is a linear constraint, P1.2.2.1 is a convex optimization problem as $\partial^2 U / \partial \mathbf{F}^2 \leq 0$. However, for tasks who are offloaded to RSU m , \mathbf{F} are highly coupled with each other. In other words, if the resource allocation of one of the tasks is increased, the resource allocation of other tasks will decrease. Therefore, we construct Lagrangian function and iteratively approach a optimal solution.

$$\begin{aligned} \mathcal{L}(\mathbf{F}, \boldsymbol{\lambda}, \boldsymbol{\mu}, \boldsymbol{\theta}) &= \sum_{k \in \mathcal{K}} \log(1 + \alpha a_{km} + \beta b_{km}) - \sum_{k \in \mathcal{K}} \lambda_k \\ &\quad \times \left(\sum_{m \in \mathcal{M}} y_{km} t_{km} - T_k^{max} \right) + \sum_{k \in \mathcal{K}} \sum_{m \in \mathcal{M}} \mu_{km} (y_{km} f_{km} - F_V) \\ &\quad - \sum_{m \in \mathcal{M}} \theta_m \left(\sum_{k \in \mathcal{K}} y_{km} f_{km} - F_m \right). \end{aligned} \quad (54)$$

where λ , μ and θ are the Lagrangian multipliers. The Lagrangian dual function (i.e., the objective dual problem) is then formulated as:

$$\mathcal{D}(\lambda, \mu, \theta) = \max \mathcal{L}(\mathbf{F}, \lambda, \mu, \theta). \quad (55)$$

Further, the object is to minimize the dual function over Lagrangian multiplier λ , μ and θ . Thus, the dual problem of P1.2.2.1 is given by:

$$\begin{aligned} \min \mathcal{D}(\lambda, \mu, \theta) \\ \text{s.t. } \lambda \geq 0, \mu \geq 0, \theta \geq 0. \end{aligned} \quad (56)$$

According to Lemma 2, P1.2.2.1 is convex as $\partial^2 U / \partial \mathbf{F}^2 \leq 0$, Therefore, there exists a strictly feasible point, and Slater's condition holds, which leads to strong duality [42]. Then, we can solve the primal problem P1.2.2.1 via the dual problem (55), which can be solved applying the gradient method. As the Lagrange function is differentiable, we can obtain the gradients of the Lagrange multipliers as:

$$\begin{aligned} \frac{\partial \mathcal{L}(\mathbf{F}, \lambda, \mu, \theta)}{\partial \lambda_k} &= - \sum_{m \in \mathcal{M}} y_{km} t_{km} + T_k^{max}; \\ \frac{\partial \mathcal{L}(\mathbf{F}, \lambda, \mu, \theta)}{\partial \mu_{km}} &= y_{km} f_{km} - F_v; \\ \frac{\partial \mathcal{L}(\mathbf{F}, \lambda, \mu, \theta)}{\partial \theta_m} &= - \sum_{k \in \mathcal{K}} y_{km} f_{km} + F_m. \end{aligned} \quad (57)$$

Further, the Lagrangian multipliers are calculated iteratively as:

$$\begin{aligned} \lambda_k(\psi + 1) &= \left[\lambda_k(j) + \varphi_1 \frac{\partial \mathcal{L}}{\partial \lambda_k} \right]^+; \\ \mu_{km}(\psi + 1) &= \left[\mu_{km}(j) + \varphi_2 \frac{\partial \mathcal{L}}{\partial \mu_{km}} \right]^+; \\ \theta_m(\psi + 1) &= \left[\theta_m(j) + \varphi_3 \frac{\partial \mathcal{L}}{\partial \theta_m} \right]^+, \end{aligned} \quad (58)$$

where ψ denotes the gradient number, $\varphi_1, \varphi_2, \varphi_3 > 0$ are the gradient steps. $[]^+$ represents $\max(0, \cdot)$. The first-order derivative of \mathcal{L} with respect to f_{km} is:

$$\begin{aligned} \frac{\partial \mathcal{L}(\mathbf{F}, \lambda, \mu, \theta)}{\partial f_{km}} &= \frac{y_{km} \beta \tilde{c}_k f_{km}^{-2}}{\ln(2) T_k^{max} (1 + \alpha a_{km} + \beta b_{km})} \\ &\quad + \frac{\lambda_k y_{km} \tilde{c}_k}{f_{km}^2} + \mu_{km} y_{km} - \theta_m y_{km}. \end{aligned} \quad (59)$$

By setting (59) to zero, we can obtain $\mathbf{F}^* = \{f_{km}^* | \forall k \in \mathcal{K}, m \in \mathcal{M}\}$.

(2) *Offloading Ratio and Transmit Power*: We can obtain the optimal computation resource allocation under given $\boldsymbol{\rho}$ and \mathbf{P} . On the contrary, the offloading ratio and transmit power problem for the given \mathbf{P} is denoted as

$$\begin{aligned} P1.2.2.2: \max_{\boldsymbol{\rho}, \mathbf{P}} U \\ \text{s.t. (11), (25b), (25e) and (25f)}. \end{aligned} \quad (60)$$

According to Lemma 1, P1.2.2.2 is non-convex problem. The process of solving this problem is the same as that of P1.2.1 in Section IV-B1. Due to limited space of this paper, we will not repeat it here. Referring to Section IV-B1, we can get the optimal solution $\boldsymbol{\rho}^*$ and \mathbf{P}^* in same way.

Algorithm 2 Joint Optimization of Energy Consumption and Task Processing Delay (JOET)

- 1: **Initialization**: Let $\phi = 1$; Initialize selection decisions $\mathbf{z}^{(0)}$, computation resources $\mathbf{F}^{(0)}$, offloading ratio $\boldsymbol{\rho}^{(0)}$ and transmit power $\mathbf{P}^{(0)}$.
- 2: **repeat**
- 3: /* Optimization of Selection Decisions */
- 4: Under given $\mathbf{F}^{(0)}$, $\boldsymbol{\rho}^{(\phi-1)}$ and $\mathbf{P}^{(\phi-1)}$, derive $\mathbf{z}^{(\phi-1)}$ by Solving P1.1 with Algorithm 1.
- 5: /* Joint Optimization of Resource Allocation, Offloading Ratio and Transmit Power */
- 6: **if** $\sum_{m \in \mathcal{M}} y_{km} = 1$ **then**
- 7: /* Offloading to the server by the vehicle relay */
- 8: Let $\psi = 1$; Initialize Lagrangian multipliers $\lambda(0)$, $\mu(0)$ and $\theta(0)$;
- 9: **repeat**
- 10: Update Lagrangian multipliers $\lambda(\psi)$, $\mu(\psi)$ and $\theta(\psi)$ based on (58);
- 11: Then determine $\mathbf{F}^{(\psi)}$ via calculating $\partial \mathcal{L}(\mathbf{F}, \lambda, \mu, \theta) / (\partial f_{km}) = 0$ based on (59)
- 12: $\psi = \psi + 1$
- 13: **until** Convergence
- 14: **end if**
- 15: Derive Offloading Ratio $\boldsymbol{\rho}^{(\psi)}$ and Transmit Power $\mathbf{P}^{(\psi)}$ by (48) and (50) respectively.
- 16: $\phi = \phi + 1$
- 17: **until** Convergence

C. JOET: Joint Optimization for Energy Consumption and Task Processing Delay

According to the discussion of previous subsections, we can efficiently solve subproblems of P1 in a distributed manner. Specifically, in order to minimize energy consumption and task processing delay, we decouple P1 into optimization of selection decisions and optimization of computation resources, offloading ratio and transmit power. That is, under given \mathbf{P} , $\boldsymbol{\rho}$ and \mathbf{P} , the VNO derives \mathbf{z} for each u_k . Further, \mathbf{F} is obtained under given \mathbf{z} , $\boldsymbol{\rho}$ and \mathbf{P} by Lagrangian method and then $\boldsymbol{\rho}$ and \mathbf{P} , is derived under given \mathbf{z} and \mathbf{F} , and repeat this process until convergence.

In Algorithm 2, since the computational complexity for solving problem P1.1 is only polynomial in convergence factor ϵ , the computational complexity required to solve P1.1 is $\mathcal{O}(\log(1/\epsilon))$. For j iterations, the complexity of the inner loop of Algorithm 2 is $\mathcal{O}(j)$. Finally, the total complexity of the Algorithm 2 is $\mathcal{O}(\phi(3 + \psi + \log(1/\epsilon)))$. Different from Ref. [30], offloading the load is only the second subproblem of this paper. In addition, this paper not only considers the return result in detail, but also optimizes the energy consumption.

V. PERFORMANCE ANALYSIS

This section demonstrates extensive simulations to evaluate the performance of the proposed JOET scheme.

A. Simulation Environment

Considering a $3\text{km} \times 3\text{km}$ square area, which consists of 25 small areas. There are 6 RSUs evenly located in the square

area. Each RSU is equipped with a VEC server. The total computation resources of the VEC servers are $F_m = 5\text{GHz}$, $\forall m \in \mathcal{M}$. Since in-vehicle applications also require computation resources, it is assumed that free resources $F_V = 1.0\text{GHz}$ and $\bar{v} = 60\text{km/h}$ for each vehicle; In the 15 small areas on the left, each small area has two IoTDs, and in the 10 small areas on the right, each small area has a IoTD, so $K=40$. Each IoTD has a computation task in each time slot $n \in \mathcal{N}$, where $N = 60$, $\delta_t = 1\text{s}$. In all computation tasks, input data size, output data size, local computation resources and the required computation resources are evenly distributed in the range of $U[10,640]\text{KB}$, $U[5,300]\text{KB}$, $U[0.1,1]\text{GHz}$ and $U[0.2,2]\text{GHz}$, respectively. Besides, the maximum processing delay and the maximum energy consumption are 1.15 times of the case that the task is computed locally, and the convergence factor $\epsilon = 0.1$. The other parameters are summarized in TABLE I.

To better evaluate the effectiveness of JOET scheme, we introduce several other benchmark schemes as follows.

1) *No Vehicle design (NoVeh)*: In this scheme, computation tasks of IoTDs can only be computed by themselves or offloaded to the VEC server without vehicle assistance;

2) *No VEC server design (NoVEC)*: In this scheme, computation tasks of IoTDs can only be computed by themselves or offloaded to the vehicle.

3) *Only relaying design (OnlyR)*: In this scheme, the vehicle can only act as a relay to assist the task transmission from the IoTD to the VEC server [9].

4) *Selection Optimization (SO)*: In this scheme, the best VEC server with maximal system utility is selected by each vehicle under a given computation resources ($f_{km} = 1.2\text{G}$) and max transmit power. Then the server allocates evenly the remaining resources to u_k s selecting the server [30].

5) *Computation Resources and Transmit Power (CRTP)*: In this scheme, computation resources and transmit power are jointly optimized. Herein, u_k offload the task to the nearest VEC servers as CRTP does not consider VEC server selection. This scheme is similar to Ref. [22], which jointly optimizes resource allocation and offloading ratio.

6) *Exhaustive Search Method (ESM)*: In this scheme, at least $(M + 1)^K (\frac{F_m}{\Delta_f})^K (\frac{F_m}{\Delta_p})^K (\frac{1}{\Delta_g})^K$ combinations of offloading schemes are evaluated to find out the optimal solution with highest utility. Δ_f , Δ_p and Δ_g are the stride step in exhaustion. Because of the enormous computational complexity, it takes a huge amount of time to run this method, so we only conduct a experiment via pruning in Section V-G.

B. Evaluation measure

Ref. [30] adopts the number of tasks to evaluate the load balancing of servers. However, when the differences (required computation resources, maximum task processing delay, etc.) among each task vary greatly, this method is difficult to measure load balancing between servers. Therefore, we propose an approach which adopts the variance of the average resource utilization efficiency to better evaluate load balancing, where the average resource utilization efficiency is denoted as $\rho_m = \frac{1}{M_m} \sum_{i=1}^{M_m} \frac{\tilde{c}_k}{f_{km}}$. Further, the variance is

calculated by:

$$s^2 = \frac{1}{M} \sum_{m \in \mathcal{M}} (\rho_m - \bar{\rho}_m)^2. \quad (61)$$

In particular, if s^2 is smaller, it indicates that the total resources required for tasks offloaded to each server are closer to the average, which makes the most fair load allocation.

C. System Utility

Firstly, we compare system utility with respect to time slot under six schemes. Fig. 3 shows JOET always achieves the greatest system utility. In Fig. 3(a), the average system utility of JOET and the other six schemes are 46.068, 43.357, 41.203, 32.838, 42.636 and 22.489 respectively. System utility of JOET is 6.25% higher than CRTP. In Fig. 3(b), six schemes are 174.78, 250.96, 213.12, 234.26, 253.52 and 253.53, respectively. System utility of JOET is basically same as that of CRTP. This is because JOET and CRTP in order to minimize energy consumption, and the both offload tasks to vehicles or servers as much as possible and optimize transmit power. In Fig. 3(c), six schemes are 173.375, 203.64, 201.20, 213.57, 223.55 and 231.41, respectively. It can be observed that the result is similar to Fig. 3(b) and other five schemes underperformer JOET. This is because these schemes often ignore one optimization object when they focus on optimizing another optimization object (energy consumption or task processing delay). In addition, system utility of six schemes fluctuates as time goes on. This is because all schemes only consider the maximum system benefit of the current time slot, but do not consider random arrival of tasks and vehicles and dynamic energy harvesting process. We will consider these important factors in future research works.

D. Energy Consumption and Task Processing Delay

In this section, we compare energy consumption and task processing delay of six schemes. Fig. 4(a) shows that the average energy consumption of NoVeh, NoVEC, OnlyR, SO, CRTP and JOET are 0.447, 0.221, 0.472, 0.339, 0.348 and 0.285, respectively. The proposed JOET reduces 15.93% compared with SO. Note that, although NoVEC achieves the lowest energy consumption, the task processing delay is greatly increased (as shown in Fig. 4(a)). This is because NoVEC cannot allocate more computation resources without VEC to effectively reduce the task processing delay. Therefore, NoVEC cannot satisfy the latency-sensitive tasks. Similar to the system utility experiments, the system utility of JOET and CRTP are similar because both optimize jointly offloading ratio and transmit power. In addition, OnlyR and NoVeh consume more energy than SO because these schemes cannot sustainably offload tasks to the vehicle for computing, which increases task processing delay. When the time taken to offloading to the server exceeds the maximum task processing delay T^{max} , the task will be computed locally. In this case, energy consumption caused by local computation is close to the maximum energy consumption. Therefore, although OnlyR

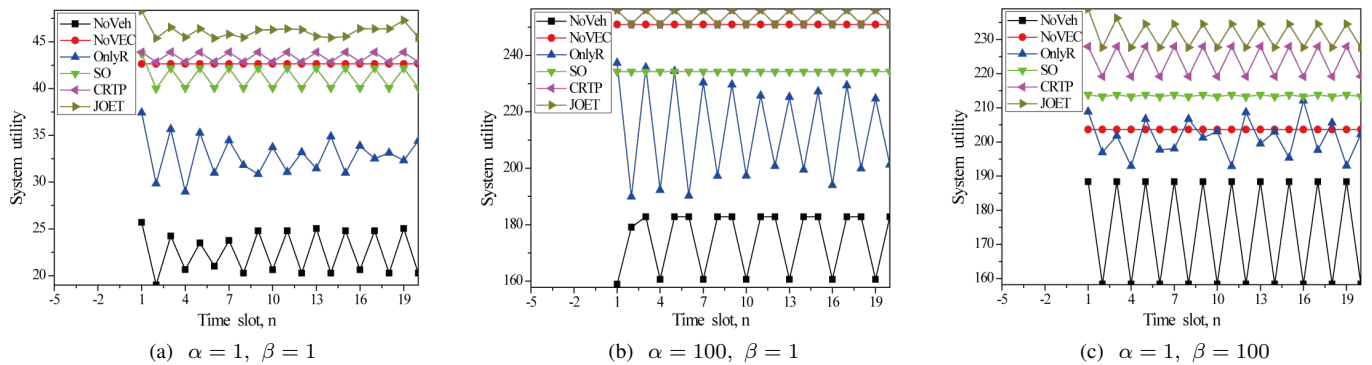


Fig. 3. Comparison of system utility with respect to time slot n under six schemes with $K = 40$ and $M = 6$ (OnlyR is from Ref. [9]; SO is from Ref. [30]; CRTP is from Ref. [22]).

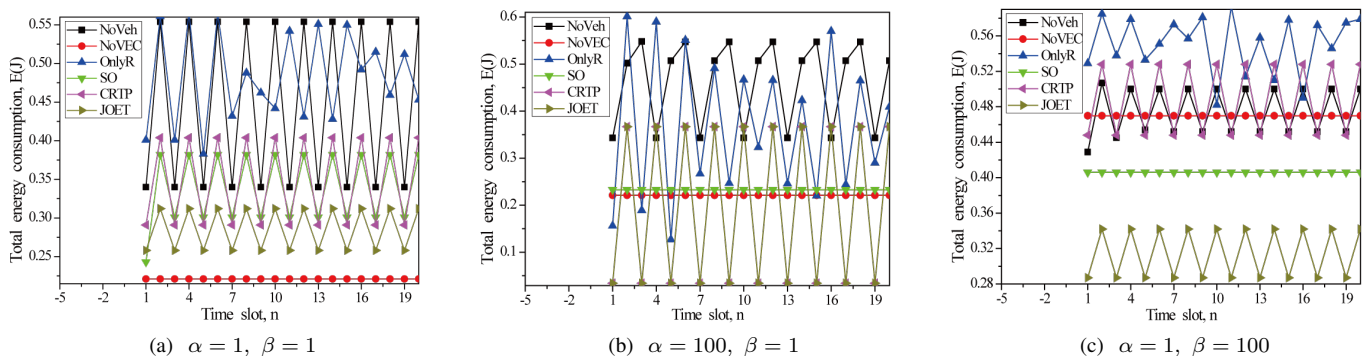


Fig. 4. Comparison of the average energy consumption under six schemes with $K = 40$ and $F_m = 5$ GHz (OnlyR is from Ref. [9]; SO is from Ref. [30]; CRTP is from Ref. [22]).

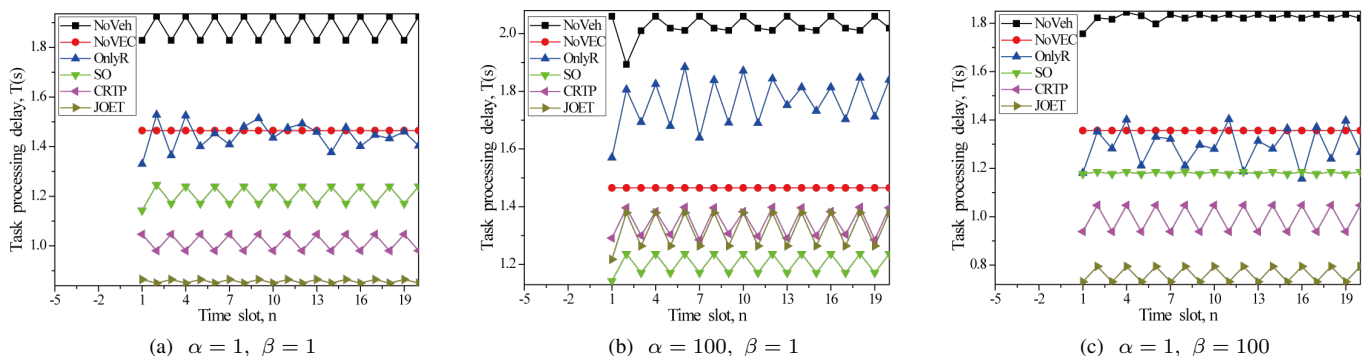


Fig. 5. Comparison of the average task processing delay under six schemes with $K = 40$ and $F_m = 5$ GHz (OnlyR is from Ref. [9]; SO is from Ref. [30]; CRTP is from Ref. [22]).

and NoVeh optimize offloading ratio and task processing delay, they are underperform SO in terms of energy consumption.

In Fig. 5(a), the average task processing delay of NoVeh, NoVEC, OnlyR, SO, CRTP and JOET are 1.876, 1.465, 1.476, 1.443, 1.204 and 1.014 respectively, where JOET reduces task processing delay by 15.78% compared to CRTP. In particular, task processing delay of NoVeh is always the greatest. This is because the task cannot be amplified and transmitted to the server through the vehicle relay without vehicle assistance, which leads to increase transmission delay. In summary, JOET minimizes task processing delay while also minimizing energy consumption through joint optimization of selection decisions, resource allocation, offloading ratio and transmit power adjust-

ment (especially in Fig. 4(c) and Fig. 5(c)).

E. Convergence

In the above two sections, we have proved that the proposed JOET outperforms the other five schemes. Furthermore, in this section, we take a convergence experiment at different initial points to verify the feasibility of JOET. In the experiment, we conduct a task requiring 1.8 GHz resources as an example. As shown in Fig. 6, it illustrates convergent evolution of the inner loop of Algorithm 2, i.e., the loop from step 9 to step 13. In Fig. 6(a), when $\alpha = 1$ and $\beta = 1$, computation resources allocated to the task after convergence reach 2.259GHz. Since

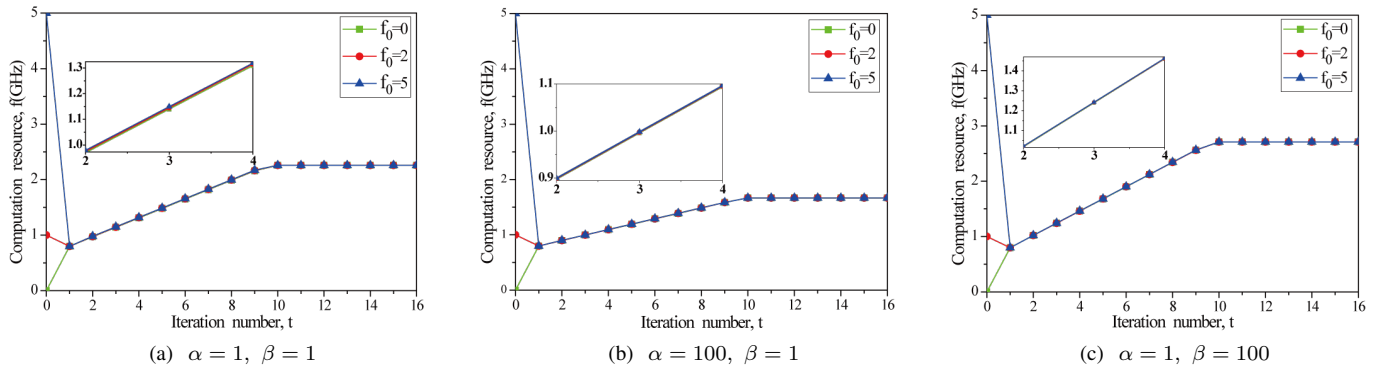


Fig. 6. The variation of computation resources allocated to the task requiring 1.8 GHz resources under different initial point with $K = 40$ and $F_m = 5$ GHz.

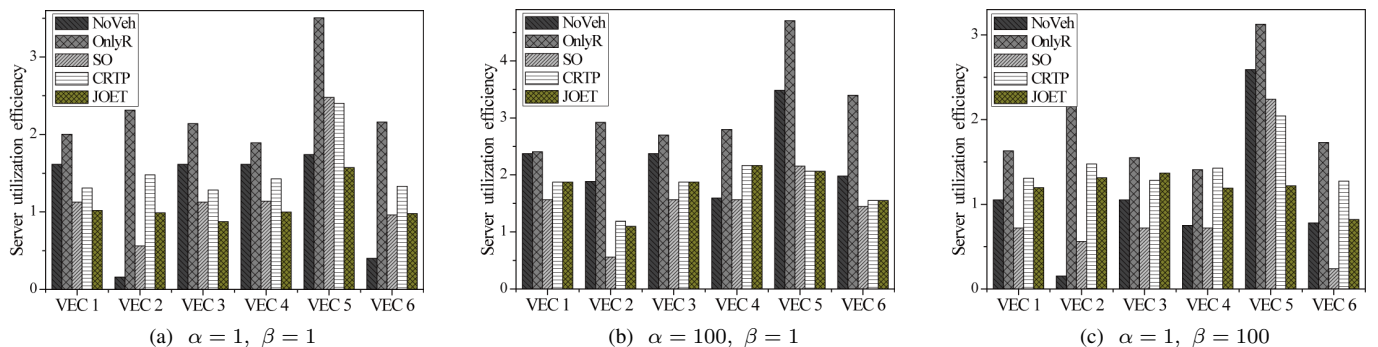


Fig. 7. Comparison of load balancing under five schemes with $K = 40$ and $F_m = 5$ GHz (OnlyR is from Ref. [9]; SO is from Ref. [30]; CRTP is from Ref. [22]).

the required resources for each task are greater than local resources, tasks that require less computation resources can be offloaded to the vehicle to greatly reduce task processing delay. Thus, the system allocates server resources to tasks that require more computation resources. In Fig. 6(b), it can be concluded that the allocated resources are only 1.668 after convergence. In order to minimize energy consumption, it is necessary to offload tasks to vehicles or servers as sustainable as possible because the communication-related energy consumption is much smaller than the computation-related energy consumption. When more tasks are assigned to the server to obtain more resources, the server can only reduce resources allocated to each task. This is different from Fig. 6(c) in that the gap between local computation delay and offloading processing delay is smaller than the gap between the computation-related energy consumption and the communication-related energy consumption. It can also be concluded that resources allocated to tasks can basically reach converge within ten iterations and converges almost simultaneously under different initial points. Thus, convergence of JOET algorithm is similar to the result of Fig. 6. Finally, it can be concluded that JOET can effectively solve the problem $P1$ based on the above results.

F. Load Balancing

In order to effectively balance the server load, JOET integrates load balancing into the task offloading problem. Different from Ref. [30], which visually presents the optimal scheme achieving the fairest load, we use the variance of

the average resource utilization efficiency reflects the server load truly. As shown in Fig. 7(a), s^2 of NoVeh, OnlyR, So, CRTP and JOET are 0.422, 0.292, 0.352, 0.154 and 0.052 respectively. JOET performs the fairest load so that the variance is the smallest and reduce 10.2% variance than CRTP. In addition, the resource utilization of OnlyR is highest. This is because the vehicle is only used as a relay to assist tasks so that more tasks are offloaded to the server for computing, which results in the highest resource utilization in OnlyR. Similar to system utility experiments, the server resource utilization of JOET and CRTP are close in Fig. 7(b). This is because the both focus on minimizing energy consumption by jointly optimizing offloading ratio and transmit power. Note that, although NoVeh and OnlyR also optimize offloading ratio and transmit power. However, NoVeh cannot access more serves without vehicle relay; OnlyR cannot offloading the task to the vehicle for computing. Therefore, the both make a unbalanced assignment of load. According to the above overview, JOET makes the fairest task assignment, which makes the load of each server as even as possible. This is because JOET does its best by integrating load balancing into VEC selection decisions. On the contrary, SO does not consider balancing server load. Although NoVeh, OnlyR and CRTP consider balancing the server load, NoVeh cannot get vehicle assistance; OnlyR only considers the vehicle as a relay; CRTP is sensitive to outliers because it only selects nearby server. Through the above experiments, the proposed JOET effectively offloads tasks with consideration of load balancing.

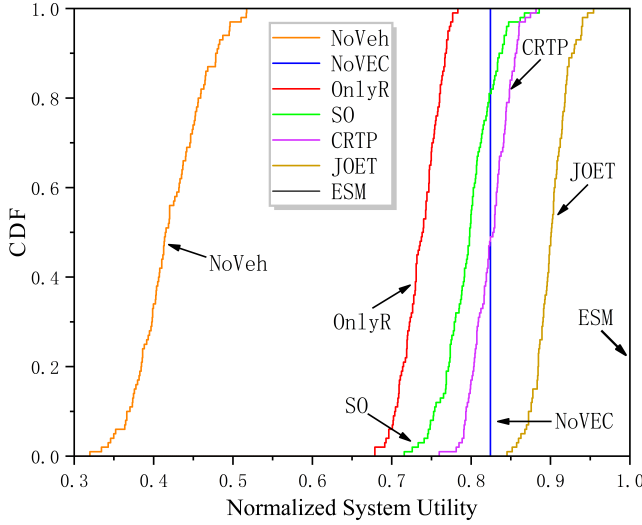


Fig. 8. Variation of system utility under different schemes with $K = 40$ and $M = 6$. (OnlyR is from Ref. [9]; SO is from Ref. [30]; CRTP is from Ref. [22]).

G. Engineering Applications

We will focus on dynamics and randomness making vehicle-assisted VEC more complex in future work. But before that, we study a preliminary random task generation. In the previous experiments, the tasks generated by IoTDs are fixed. In order to evaluate the generalization ability of these offloading schemes, we analyze the performance of each schemes across different simulation runs that randomly generate different tasks for each IoTd. In simulation run, the system utility of each scheme is normalized, which is presented as a ratio of the system utility to the optimal one obtained by ESM. Obviously, the ratio cannot be greater than 1, and the ESM performs 1 in each simulation run. We adopt the Cumulative Distribution Function (CDF) to present the distribution of the ratios across all the simulation runs [14] when all tasks from IoTDs are randomly generated. As shown in Fig. 8, the utility ratio of NoVEC is always equal to 0.824. This is because NoVEC always offloads tasks to vehicles and thus achieves the same system utility, which is consistent with Fig. 3. Similarly, NoVeh achieves the lower system utility because of random task assignment. In Fig. 3, SO and CRTP are close to JOET. However, due to the random task assignment, SO without optimization of resources cannot make better selection decisions, and CRTP that offloads nearby tasks cannot meet more requirement of tasks. JOET performs the better generalization ability by jointly optimizing selection decisions, resource allocation, offloading ratio and transmit power adjustment.

VI. CONCLUSION AND FUTURE WORK

In this paper, we investigated a sustainable vehicle-assisted VEC system, where the vehicle not only can compute the latency-sensitive tasks, but also act as a relay to help tasks from IoTDs to VEC servers. We proposed integrating load balancing with the offloading problem to efficiently complete tasks and further formulate the problem as a mix-integer non-linear optimization problem. By employing decomposition, the problem is decoupled into two separable subproblems, and

finally solve the original problem by solving subproblems iteratively. In summary, we proposed a joint optimization energy consumption and task processing delay scheme, called JOET, which aims to sustainably reduce the total energy consumption and task processing delay via jointly optimizing selection decisions, computation resource allocation, offloading ratio and transmit power adjustment. Finally, we conducted extensive simulation experiments. The results show that our proposed JOET minimizes energy consumption and task processing delay while performing a fairer task assignment than other schemes.

For the future work, because the vehicle-assisted system does not consider randomization and dynamics, that is, random arrival of tasks and vehicles and dynamic energy harvesting process, which makes the optimization problem more arduous, we will pour attention to dynamics and randomization to make the offloading scheme in sustainable vehicle-assisted VEC system more feasible.

APPENDIX A PROOF OF THE LEMMA 1

The second-order derivative of U with respect to \boldsymbol{q} is:

$$\frac{\partial^2 U}{\partial \boldsymbol{q}^2} = -\frac{1}{\ln(2)} \frac{\beta}{T_k^{max}} \frac{\omega_3'}{\omega_0} - \frac{1}{\ln(2)} \left(\frac{I_k}{R_k^{k \rightarrow v}} \omega_1 + \omega_2 + \omega_3 \right)^2, \quad (62)$$

where ω_1 , ω_2 and ω_3 are defined in (46), $\omega_3' = \frac{(2+\omega_3)\bar{c}_k \bar{v}}{(1+\frac{p_v \xi_1}{d_{vv}^2}) R_k^{v \rightarrow v} d_{vv}^3 F_V} \times (\frac{4B_0 p_v \xi_1}{\ln(2)} - (3d_{vv}^2 + p_v \xi_1) R_k^{v \rightarrow v})$.

Obviously, $d_{vv} > 1$, but $\frac{4B_0 p_v \xi_1}{\ln(2)} - (3d_{vv}^2 + p_v \xi_1) R_k^{v \rightarrow v}$ is indefinite. Further,

$$\frac{\partial^2 U}{\partial \boldsymbol{q} \partial \boldsymbol{P}} = \frac{\partial^2 U}{\partial \boldsymbol{P} \partial \boldsymbol{q}} = -\frac{\omega_0^{-2}}{\ln(2)} \left(\frac{\alpha I_k}{\eta E_k^{max} R_k^{k \rightarrow v}} - \omega_1 \omega_4 \right) \times [\omega_0 + \varrho_k \left(\frac{I_k \omega_1}{R_k^{k \rightarrow v}} + \omega_2 \right)], \quad (63)$$

where $\omega_4 = \frac{I_k \frac{\xi_0}{d_{kv}^2} B_0 (R_k^{k \rightarrow v})^{-2}}{\ln(2) (1 + \frac{p_k \xi_0}{d_{kv}^2})}$. Further,

$$\frac{\partial^2 U}{\partial \boldsymbol{P}^2} = -\frac{1}{\ln(2)} \frac{\omega_4 \varrho_k (\omega_1 \omega_5 - \frac{2\alpha}{\eta E_k^{max}})}{\omega_0} - \frac{1}{\ln(2)} \left(\frac{\alpha}{\eta E_k^{max}} \frac{\varrho_k I_k}{R_k^{k \rightarrow v}} - \omega_1 \omega_4 \varrho_k \right)^2, \quad (64)$$

where $\omega_5 = \frac{\xi_0}{d_{kv}^2 (1 + \frac{p_k \xi_0}{d_{kv}^2})} (1 + \frac{2B_0}{\ln(2) R_k^{k \rightarrow v}})$. Then,

$$\begin{aligned} \frac{\partial^2 U}{\partial \boldsymbol{q}^2} \frac{\partial^2 U}{\partial \boldsymbol{P}^2} - \frac{\partial^2 U}{\partial \boldsymbol{q} \partial \boldsymbol{P}} \frac{\partial^2 U}{\partial \boldsymbol{P} \partial \boldsymbol{q}} &= \frac{1}{(\ln(2) \omega_0^2)^2} \\ &\times \left[\frac{\beta \omega_0 \omega_3' \varrho_k}{T_k^{max}} \times (\omega_0 \omega_4 (\omega_1 \omega_5 - \frac{2\alpha}{\eta E_k^{max}}) + \frac{\alpha}{\eta E_k^{max}} \frac{\varrho_k I_k}{R_k^{k \rightarrow v}} \right. \\ &- \omega_1 \omega_4 \varrho_k) + \left(\frac{I_k \omega_1}{R_k^{k \rightarrow v}} + \omega_2 + \omega_3 \right)^2 (\omega_0 \omega_4 (\omega_1 \omega_5 - \frac{2\alpha}{\eta E_k^{max}}) \\ &+ \frac{\alpha}{\eta E_k^{max}} \frac{\varrho_k I_k}{R_k^{k \rightarrow v}} - \omega_1 \omega_4 \varrho_k) - \left(\frac{I_k}{R_k^{k \rightarrow v}} \omega_1 + \omega_2 \right)^2 \\ &\times \left(\frac{\alpha}{\eta E_k^{max}} \frac{\varrho_k I_k}{R_k^{k \rightarrow v}} - \omega_1 \omega_4 \varrho_k \right)^2 - 2\omega_0 \varrho_k \left(\frac{I_k}{R_k^{k \rightarrow v}} \omega_1 + \omega_2 \right) \end{aligned}$$

$$\times \left(\frac{\alpha I_k}{\eta E_k^{max} R_k^{k \rightarrow v}} - \omega_1 \omega_4 \right)^2 - \omega_0^2 \left(\frac{\alpha I_k}{\eta E_k^{max} R_k^{k \rightarrow v}} - \omega_1 \omega_4 \right)^2 \Big]. \quad (65)$$

According to the Section V-A and Table I, we have $\omega_0, \omega_1, \omega_3, \omega_4, \omega_5 > 0$, but ω_2 is indefinite because $F_k - F_V$ is indefinite.

$$\begin{aligned} \omega_1 \omega_5 &> \frac{2\alpha}{\eta E_k^{max}} \frac{\frac{\xi_0 B_0}{\ln(2)} (p_k + \vartheta_{k,c})}{d_{kv}^2 R_k^{k \rightarrow v} (1 + \frac{p_k \xi_0}{d_{kv}^2})} \\ &= \frac{2\alpha}{\eta E_k^{max}} \frac{\frac{\xi_0}{d_{kv}^2} (p_k + \vartheta_{k,c})}{\ln(2) (1 + \frac{p_k \xi_0}{d_{kv}^2}) \log(1 + \frac{p_k \xi_0}{d_{kv}^2})} \\ &> \frac{2\alpha}{\eta E_k^{max}} \frac{x + \frac{1}{8}x}{\ln(2) (1 + x) \log(1 + x)} > \frac{2\alpha}{\eta E_k^{max}}, \quad (66) \end{aligned}$$

where $0 < x \ll 1$. However, the formula (65) still is indefinite. P1.2.1 is nonconvex optimization problem [30], [42].

APPENDIX B

PROOF OF THE LEMMA 2

In P1.2.1, we use the extreme value discriminant in the multivariate function to check its convexity [42]. Next, we calculate the second-order derivative of each variable in turn.

The second-order derivative of U with respect to \mathbf{F} is:

$$\frac{\partial^2 U}{\partial \mathbf{F}^2} = - \frac{y_{km} \beta \varrho_k \tilde{c}_k}{\ln(2) T_k^{max} f_{km}^3 \omega_0^2} \left(\omega_0 + \frac{y_{km} \beta \tilde{c}_k}{T_k^{max} f_{km}} \right). \quad (67)$$

The second-order derivative of U with respect to \mathbf{F} and \mathbf{P} is given by:

$$\begin{aligned} \frac{\partial^2 U}{\partial \mathbf{F} \partial \mathbf{P}} &= \frac{\partial^2 U}{\partial \mathbf{P} \partial \mathbf{F}} = \frac{y_{km} \beta \varrho_k^2 \tilde{c}_k}{\ln(2) T_k^{max} f_{km}^2 \omega_0^2} \\ &\times \left(\frac{\alpha I_k}{\eta E_k^{max} R_k^{k \rightarrow v}} - \omega_1 \omega_3 \right). \quad (68) \end{aligned}$$

The second-order derivative of U with respect to \mathbf{F} and ϱ is denoted as:

$$\begin{aligned} \frac{\partial^2 U}{\partial \mathbf{F} \partial \varrho} &= \frac{\partial^2 U}{\partial \varrho \partial \mathbf{F}} = \frac{y_{km} \beta \tilde{c}_k}{\ln(2) T_k^{max} f_{km}^2 \omega_0^2} \\ &\times \left(\omega_0 + \varrho_k \left(\frac{I_k}{R_k^{k \rightarrow v}} \omega_1 + \frac{I_k}{R_k^{v \rightarrow m}} + \omega_2 \right) \right). \quad (69) \end{aligned}$$

Combining with (62), (63) and (64) in Lemma 1, the Hessian matrix of P1.2.2 is expressed as:

$$H(U) = \begin{bmatrix} \frac{\partial^2 U}{\partial \varrho^2} & \frac{\partial^2 U}{\partial \varrho \partial \mathbf{P}} & \frac{\partial^2 U}{\partial \varrho \partial \mathbf{F}} \\ \frac{\partial^2 U}{\partial \mathbf{P} \partial \varrho} & \frac{\partial^2 U}{\partial \mathbf{P}^2} & \frac{\partial^2 U}{\partial \mathbf{P} \partial \mathbf{F}} \\ \frac{\partial^2 U}{\partial \mathbf{F} \partial \varrho} & \frac{\partial^2 U}{\partial \mathbf{F} \partial \mathbf{P}} & \frac{\partial^2 U}{\partial \mathbf{F}^2} \end{bmatrix}. \quad (70)$$

Note that, $\frac{\partial^2 U}{\partial \varrho^2} = -\frac{1}{\ln(2)} \left(\frac{\frac{I_k \omega_1}{R_k^{k \rightarrow v}} + \omega_2}{\omega_0} \right)^2 < 0$ is slightly changed with respect to (62) because $t_k^{k \rightarrow v}$ is different from $t_k^{k \rightarrow m}$ (same for ω_2 and $\frac{\partial^2 U}{\partial \varrho \partial \mathbf{P}}$). However, the conclusion is the consistent. According to the property of Hessian matrix [44]. The necessary and sufficient condition for P1.2.2 is that the matrix $H(U)$ is at least positive semi-definite. However, it can be obtained that $\frac{\partial^2 U}{\partial \varrho^2} \frac{\partial^2 U}{\partial \mathbf{P}^2} - \frac{\partial^2 U}{\partial \varrho \partial \mathbf{P}} \frac{\partial^2 U}{\partial \mathbf{P} \partial \varrho}$ is indefinite based on Lemma 2. Thus, P1.2.2 is also non-convex.

ACKNOWLEDGMENT

This work was supported in part by the National Natural Science Foundation of China (No. 62072475, No. 61772554).

REFERENCES

- [1] S. R. Pookhrel and J. Choi, "Improving tcp performance over wifi for internet of vehicles: A federated learning approach," *IEEE Transactions on Vehicular Technology*, vol. 69, no. 6, pp. 6798–6802, 2020.
- [2] H. Vasudev, V. Deshpande, D. Das, and S. K. Das, "A lightweight mutual authentication protocol for v2v communication in internet of vehicles," *IEEE Transactions on Vehicular Technology*, vol. 69, no. 6, pp. 6709–6717, 2020.
- [3] X. Zhu, Y. Luo, A. Liu, M. Z. A. Bhuiyan, and S. Zhang, "Multiagent deep reinforcement learning for vehicular computation offloading in iot," *IEEE Internet of Things Journal*, vol. 8, no. 12, pp. 9763–9773, 2020.
- [4] B. Marr, "How much data do we create every day? the mind-blowing stats everyone should read," in *Forbes*, 2018, pp. 1–5.
- [5] H. Teng, M. Dong, Y. Liu, W. Tian, and X. Liu, "A low-cost physical location discovery scheme for large-scale internet of things in smart city through joint use of vehicles and uavs," *Future Generation Computer Systems*, vol. 118, pp. 310–326, 2021.
- [6] U. Cisco, "Cisco annual internet report (2018–2023) white paper," *Online* (accessed March 26, 2021) <https://www.cisco.com/c/en/us/solutions/collateral/executive-perspectives/annual-internet-report/whitepaper-c11-741490.html>, 2020.
- [7] X. Zhu, Y. Luo, A. Liu, W. Tang, and M. Z. A. Bhuiyan, "A deep learning-based mobile crowdsensing scheme by predicting vehicle mobility," *IEEE Transactions on Intelligent Transportation Systems*, 2020.
- [8] K. L. Lueth *et al.*, "State of the iot 2018: Number of iot devices now at 7b—market accelerating," *IoT Analytics*, vol. 8, 2018.
- [9] W. Huang, K. Ota, M. Dong, T. Wang, S. Zhang, and J. Zhang, "Result return aware offloading scheme in vehicular edge networks for iot," *Computer Communications*, vol. 164, pp. 201–214, 2020.
- [10] U. Saleem, Y. Liu, S. Jangsher, X. Tao, and Y. Li, "Latency minimization for d2d-enabled partial computation offloading in mobile edge computing," *IEEE Transactions on Vehicular Technology*, vol. 69, no. 4, pp. 4472–4486, 2020.
- [11] S. Huang, Z. Zeng, K. Ota, M. Dong, T. Wang, and N. N. Xiong, "An intelligent collaboration trust interconnections system for mobile information control in ubiquitous 5g networks," *IEEE Transactions on Network Science and Engineering*, vol. 8, no. 1, pp. 347–365, 2020.
- [12] M. Bonola, L. Bracciale, P. Loreti, R. Amici, A. Rabuffi, and G. Bianchi, "Opportunistic communication in smart city: Experimental insight with small-scale taxi fleets as data carriers," *Ad Hoc Networks*, vol. 43, pp. 43–55, 2016.
- [13] M. Shen, A. Liu, G. Huang, N. N. Xiong, and H. Lu, "Attcd: An active and traceable trust data collection scheme for industrial security in smart cities," *IEEE Internet of Things Journal*, vol. 8, no. 8, pp. 6437–6453, 2021.
- [14] W. Zhan, C. Luo, G. Min, C. Wang, Q. Zhu, and H. Duan, "Mobility-aware multi-user offloading optimization for mobile edge computing," *IEEE Transactions on Vehicular Technology*, vol. 69, no. 3, pp. 3341–3356, 2020.
- [15] C. Zhou, Y. Gu, S. He, and Z. Shi, "A robust and efficient algorithm for coprime array adaptive beamforming," *IEEE Transactions on Vehicular Technology*, vol. 67, no. 2, pp. 1099–1112, 2017.
- [16] C. Liu, K. Liu, S. Guo, R. Xie, V. C. Lee, and S. H. Son, "Adaptive offloading for time-critical tasks in heterogeneous internet of vehicles," *IEEE Internet of Things Journal*, vol. 7, no. 9, pp. 7999–8011, 2020.
- [17] S. Huang, A. Liu, S. Zhang, T. Wang, and N. Xiong, "Bd-vte: A novel baseline data based verifiable trust evaluation scheme for smart network systems," *IEEE Transactions on Network Science and Engineering*, 2020.
- [18] C.-F. Liu, M. Bennis, M. Debbah, and H. V. Poor, "Dynamic task offloading and resource allocation for ultra-reliable low-latency edge computing," *IEEE Transactions on Communications*, vol. 67, no. 6, pp. 4132–4150, 2019.
- [19] H. Shiri, J. Park, and M. Bennis, "Communication-efficient massive uav online path control: Federated learning meets mean-field game theory," *IEEE Transactions on Communications*, vol. 68, no. 11, pp. 6840–6857, 2020.

- [20] Y. ZHANG and Z. WANG, "Hybrid malware detection approach with feedback-directed machine learning," *Information Sciences*, vol. 63, no. 139103, pp. 1–139 103, 2020.
- [21] C. Zhou, Y. Gu, X. Fan, Z. Shi, G. Mao, and Y. D. Zhang, "Direction-of-arrival estimation for coprime array via virtual array interpolation," *IEEE Transactions on Signal Processing*, vol. 66, no. 22, pp. 5956–5971, 2018.
- [22] Y. Yu, J. Zhang, and K. B. Letaief, "Joint subcarrier and cpu time allocation for mobile edge computing," in *2016 IEEE Global Communications Conference (GLOBECOM)*. IEEE, 2016, pp. 1–6.
- [23] M. Yu, A. Liu, N. N. Xiong, and T. Wang, "An intelligent game based offloading scheme for maximizing benefits of iot-edge-cloud ecosystems," *IEEE Internet of Things Journal*, 2020.
- [24] M. Al-Khafajiy, T. Baker, M. Asim, Z. Guo, R. Ranjan, A. Longo, D. Puthal, and M. Taylor, "Comitment: a fog computing trust management approach," *Journal of Parallel and Distributed Computing*, vol. 137, pp. 1–16, 2020.
- [25] K. Xu, L. Lv, T. Li, M. Shen, H. Wang, and K. Yang, "Minimizing tardiness for data-intensive applications in heterogeneous systems: A matching theory perspective," *IEEE Transactions on Parallel and Distributed Systems*, vol. 31, no. 1, pp. 144–158, 2019.
- [26] H. Guo and J. Liu, "Uav-enhanced intelligent offloading for internet of things at the edge," *IEEE Transactions on Industrial Informatics*, vol. 16, no. 4, pp. 2737–2746, 2019.
- [27] T. Zhang, Y. Xu, J. Loo, D. Yang, and L. Xiao, "Joint computation and communication design for uav-assisted mobile edge computing in iot," *IEEE Transactions on Industrial Informatics*, vol. 16, no. 8, pp. 5505–5516, 2019.
- [28] A. Ndikumana, N. H. Tran, T. M. Ho, Z. Han, W. Saad, D. Niyato, and C. S. Hong, "Joint communication, computation, caching, and control in big data multi-access edge computing," *IEEE Transactions on Mobile Computing*, vol. 19, no. 6, pp. 1359–1374, 2019.
- [29] F. Zhou, Y. Wu, R. Q. Hu, and Y. Qian, "Computation rate maximization in uav-enabled wireless-powered mobile-edge computing systems," *IEEE Journal on Selected Areas in Communications*, vol. 36, no. 9, pp. 1927–1941, 2018.
- [30] Y. Dai, D. Xu, S. Maharjan, and Y. Zhang, "Joint load balancing and offloading in vehicular edge computing and networks," *IEEE Internet of Things Journal*, vol. 6, no. 3, pp. 4377–4387, 2018.
- [31] T. Shu, M. Krunz, and S. Vrudhula, "Joint optimization of transmit power-time and bit energy efficiency in cdma wireless sensor networks," *IEEE Transactions on Wireless Communications*, vol. 5, no. 11, pp. 3109–3118, 2006.
- [32] S. Cui, A. J. Goldsmith, and A. Bahai, "Energy-constrained modulation optimization," *IEEE transactions on wireless communications*, vol. 4, no. 5, pp. 2349–2360, 2005.
- [33] J. Ren, Y. Zhang, N. Zhang, D. Zhang, and X. Shen, "Dynamic channel access to improve energy efficiency in cognitive radio sensor networks," *IEEE Transactions on Wireless Communications*, vol. 15, no. 5, pp. 3143–3156, 2016.
- [34] J. Ren, Y. Zhang, K. Zhang, A. Liu, J. Chen, and X. S. Shen, "Lifetime and energy hole evolution analysis in data-gathering wireless sensor networks," *IEEE transactions on industrial informatics*, vol. 12, no. 2, pp. 788–800, 2015.
- [35] L. Li, T. Q. Quek, J. Ren, H. H. Yang, Z. Chen, and Y. Zhang, "An incentive-aware job offloading control framework for multi-access edge computing," *IEEE Transactions on Mobile Computing*, vol. 20, no. 1, pp. 63–75, 2019.
- [36] A. P. Miettinen and J. K. Nurminen, "Energy efficiency of mobile clients in cloud computing," *HotCloud*, vol. 10, no. 4-4, p. 19, 2010.
- [37] Q. Ye, O. Y. Bursalioglu, H. C. Papadopoulos, C. Caramanis, and J. G. Andrews, "User association and interference management in massive mimo hetnets," *IEEE Transactions on Communications*, vol. 64, no. 5, pp. 2049–2065, 2016.
- [38] L. Li, M. Pal, and Y. R. Yang, "Proportional fairness in multi-rate wireless lans," in *IEEE INFOCOM 2008-The 27th Conference on Computer Communications*. IEEE, 2008, pp. 1004–1012.
- [39] J. Kleinberg and E. Tardos, *Algorithm design*. Pearson Education India, 2006.
- [40] M. Hong, M. Razaviyayn, Z.-Q. Luo, and J.-S. Pang, "A unified algorithmic framework for block-structured optimization involving big data: With applications in machine learning and signal processing," *IEEE Signal Processing Magazine*, vol. 33, no. 1, pp. 57–77, 2015.
- [41] D. B. Shmoys and É. Tardos, "An approximation algorithm for the generalized assignment problem," *Mathematical programming*, vol. 62, no. 1, pp. 461–474, 1993.
- [42] S. Boyd, S. P. Boyd, and L. Vandenberghe, *Convex optimization*. Cambridge university press, 2004.
- [43] A. M. Awwal, P. Kumam, and A. B. Abubakar, "A modified conjugate gradient method for monotone nonlinear equations with convex constraints," *Applied Numerical Mathematics*, vol. 145, pp. 507–520, 2019.
- [44] T. Sun and S. Yang, "An approach to formulate the hessian matrix for dynamic control of parallel robots," *IEEE/ASME Transactions on Mechatronics*, vol. 24, no. 1, pp. 271–281, 2019.